THE HONG KONG
POLYTECHNIC UNIVERSITY
香港理工大學
Pao Yue-kong Library
包玉剛圖書館

Copyright Undertaking

This thesis is protected by copyright, with all rights reserved.

By reading and using the thesis, the reader understands and agrees to the following terms:

1. The reader will abide by the rules and legal ordinances governing copyright regarding the use of the thesis.
2. The reader will use the thesis for the purpose of research or private study only and not for distribution or further reproduction or any other purpose.
3. The reader agrees to indemnify and hold the University harmless from and against any loss, damage, cost, liability or expenses arising from copyright infringement or unauthorized usage.

IMPORTANT

If you have reasons to believe that any materials in this thesis are deemed not suitable to be distributed in this form, or a copyright owner having difficulty with the material being included in our database, please contact lbsys@polyu.edu.hk providing details. The Library will look into your claim and consider taking remedial action upon receipt of the written requests.

Pao Yue-kong Library, The Hong Kong Polytechnic University, Hung Hom, Kowloon, Hong Kong

http://www.lib.polyu.edu.hk

This thesis in electronic version is provided to the Library by the author. In the case where its contents is different from the printed version, the printed version shall prevail.

The Hong Kong Polytechnic University

Department of Applied Physics

SURFACE MODIFICATION OF POLYDIMETHYSILOXANE THROUGH PLASMA ION IMPLANTATION

SUN Yue

A thesis submitted in partial fulfillment of the requirements for the degree of Master of Philosophy

August 2013

CERTIFICATE OF ORIGINALITY

I hereby declare that this thesis is my own work and that, to the best of my knowledge and belief, it reproduces no material previously published or written, nor material that has been accepted for the award of any other degree or diploma, except where due acknowledgement has been made in the text.

_____ (Signed)

_____ SUN Yue_____(Name of student)

Scholarly Activities

Peer-reviewed journal publications:

1. Y. Sun, H. Y. Wang, T. Xiong, P. K. Chu and C. W. Leung, "Feature development on prepatterned elastomer surfaces upon ion implantation", *Microelectronic Engineering* **110**, 346-349 (2013).
2. H.K. Woo, Y. Sun, K.Y. Mak, C.W. Leung, Y. Du, L. Li, P. T. Lai, C. H. Leung, C. M. Wong, J. Shi and P. W. T. Pong, "Effect of O_2 -plasma treatment on nanogrooved PDMS surfaces for modulating cellular behavior of mammalian cells" (under review)

Conference presentation:

1. Y. Sun, C. W. Leung, "Control of Feature Development on Elastomer Surface during Plasma Ion Implantation by Surface Prepatterning", in *38th International Conference on Micro and Nano Engineering (MNE) 2012*, 16 Sep to 20 Sep 2012, Toulouse, France.

Abstract

Polydimethylsiloxane (PDMS) is a silicone elastomer with many attractive properties such as machinability, low cost, and resistance to corrosion in various industrial and biomedical applications, among many others. Due to the chemically-inert nature of PDMS, modifications are necessary for the introduction of various functional groups on PDMS surfaces. One of such methods is plasma implantation.

On the other hand, plasma implantation treatment can induce significant changes to the surface morphology of the samples, such as periodic rippling of surfaces in localized areas (less than hundreds of microns) that are otherwise disordered on macroscopic scales.

In this project, I investigated the development of induced ripple structures formed during the plasma treatment process. It was found that a surface prepatterning step of the PDMS surface could lead to the suppression of the wavy patterns, if the implantation voltage was small. As the plasma voltage increased, the prepatterns on PDMS could guide the development of ripple growth on the surfaces, which may be used for studying the wrinkling mechanism on elastic surfaces, and for developing surfaces with designed hierarchal sub-micron or nanometer features. The effect of

plasma implantation duration, and the influence of surface prepattern dimensions, were investigated.

To demonstrate the applications of such ion-implanted PDMS surfaces, plasma-treated samples were used as substrates for cell culturing studies for different cell types. Processing parameters (plasma bias voltage, processing time, surface prepattern features, etc.) were varied to induce different topologies on PDMS surfaces. A systematic investigation of cell culturing on the patterned surfaces was conducted. By using MC3T3-E1cells cultured on prepatterned samples, I demonstrated the importance of controlling the surface feature sizes and the depths of prepatterned features on the cell growth processes. To illustrate the biocompatibility of these prepatterned features, cell adhesion and cell proliferation experiments were performed using both MC3T3-E1 and EAhy926 cells. In addition, to evaluate the importance of patterned surfaces in inducing cell alignment, HeLa cells were cultured on hierarchal patterns formed by high-voltage implantation of hierarchal surfaces.

In summary, this work investigated the influence of surface prepatterning on the development of the topology of PDMS surfaces during plasma implantation process. Through careful control of both the surface prepatterns and the implantation conditions,

a rich variety of surface features (ranging from minimal surface corrugations to the formation of hierarchal features) were obtained, demonstrating the power of combining the two techniques in the surface topology modification of elastomer surfaces. Since the surface prepatterning steps can be easily scaled for large-scale manufacturing, it should be directly applicable for industrial-scale surface modification processes. An attempt was also made to use the treated PDMS for cell studies *in vitro*, illustrating the possibility of interdisciplinary studies using such a material system.

Acknowledgements

First of all, I would like to express my deep gratitude to my supervisor, Dr. C. W. Leung, who offered the opportunity for me to pursue my Master of Philosophy degree in the Department of Applied Physics. He is the one who gave me support, patience and encouragement when I met difficulties during the last two years. The most important was that he had good characters and a kind heart. He always has the interests of students at heart. Thank you again for your continued help, your input, academic ideas and suggestions on my project. Without your enlightenment, this thesis could not have been possible. Please accept my warmest thanks.

I would also like to thank Prof. Paul K. Chu from the Department of Physics and Materials Science at the City University of Hong Kong for his help on surface modification through plasma treatment and cell culturing experiments. My thanks extend to his group members including Mr. M. Zhang, Mr. H. Y. Wang and Mr. P. H. Li, among many others, for their kind assistance.

Heartfelt thanks as well to Dr. Gloria Xin for taking care of me during my study period. Her care has warmed my heart a lot. I am grateful for her help, sharing meaningful academic resources, providing advice and continued support from the

beginning of our friendship.

Finally, I would like to express my deepest gratitude and appreciation to my parents, my dear aunt Zhang Sumin and my sister Duan Yuanyuan. They have always been there, believed in me and understood me, especially during my graduate study period.

Table of contents

List of figures and tables

Chapter 1. INTRODUCTION

In this Chapter, the background and motivations of this project are introduced, including the interaction between polymeric materials and surface modification techniques. After this, the scope of the present study is mentioned. This thesis is divided into six chapters, and the outline for every chapter is introduced.

1.1 Background and motivations

Polymeric materials have attractive properties such as machinability, light-weightedness and high-flexibility, and are widely used in various industrial and biomedical applications [1][2][3]. For example, the capability of polymers for fabrication with rapid prototyping or stamping techniques at large scales and low costs makes them particularly attractive for micro-electromechanical or micro-fluidic systems [4][5]. Meanwhile, the increasing number of biomedical research has led to the pursuit of biocompatible materials apart from the traditional silicon-based ones. New fabrication techniques such as soft lithography [6] or nanoimprinting [7] allow shaping of such bio-friendly polymers for controlling cell growth. Polycarbonate (PC), polymethylmethacrylate (PMMA), polyethylene (PE) and polydimethylsiloxane

(PDMS) are some of polymers typically used in engineering fields. Among these, PDMS is the material heavily utilized for biomedical applications. This can be attributed to its numerous remarkable features including thermal stability, biocompatibility, elastomeric properties, ease of stamping into (sub)micro-meter features, high chemical inertness and low manufacturing cost [8][9][10][11][12].

Although PDMS has many advantages, in several applications it is necessary to modify the surface properties such as surface wettability, chemical compositions, and surface energy of the PDMS sample surface. [13]. For example, the hydrophobicity of PDMS makes it difficult to introduce liquids into microchannels of PDMS-based devices [14]. In addition, the poor adhesion limits the potential for metal-polymer or polymer-polymer contacts, as well as molding or dyeing onto PDMS [1]. Therefore, surface modification of PDMS plays a very important role, as selected surface properties can be enhanced while the bulk attributes can be maintained.

There are various PDMS surface modification methods, which can be divided into three categories: gas-phase processes, wet chemical methods and a combination of both. Gas-phase processes include plasma treatment [15][16][17], UV irradiation sputtering, and chemical vapor deposition (CVD) [18] Wet chemical methods include layer-by-layer (LBL) deposition of ions with opposite charges on flat surfaces [19], sol-

gel coatings [20] or silanization [19]. There are also reports which demonstrate surface modification by combinations of gas-phase and wet chemical methods, including silanization/LBL methods on PDMS samples pretreated with plasma oxidation or chemical oxidation [19].

Plasma-based techniques, such as plasma immersion, ion implantation and deposition (PIII&D) [21] are widely used in the surface modification of various types of engineering materials. These were shown to be an effective method to modify the physicochemical characteristics of surface layers [22]. In PIII&D, the target is typically enshrouded in self-excited plasma generated by applying a high negative voltage to the target holder. The energetic ions bombard the sample surfaces at normal incidence and penetrate more deeply into the samples than conventional surface treatment methods [23]. This process makes effective and uniform ion bombardment, which is highly desirable for treating three-dimension subjects and engineering polymers [24].

On the other hand, this technique can induce significant changes to the surface morphology of PDMS samples. In fact, many studies concerning the effects of plasma treatment on the surface pattern growth have been made, as surface texturing after plasma treatment can be applied to affect the roughness, biocompatibility, and optical properties of materials [25]. Plasma treatment on PDMS can induce periodic structures

[26], the periodicity of which can be adjusted by process parameters such as bias voltage or processing time, but the resultant patterns are generally disordered. Bowden *et a*l. [27] exposed PDMS samples patterned in bas-relief structure to oxygen plasma, in order to generate oriented ripples. Therefore, the control of surface morphology of PDMS is of great potential as it can affect the functionality of surface structures. In particular, plasma-treated PDMS samples can be used as stamps for microcontact printing of proteins on the PMMA substrates. In contrast, without plasma treatment, the protein solution beads up on the surfaces, so there is no adhesion between PDMS stamps and PMMA substrates [28]. In addition, plasma treatment is well known to influence the surface composition of polymers, to change them from hydrophobic to hydrophilic. This is favourable for the culturing of cells [29], because surface functional groups such as carboxyl, amine and hydroxyl can be formed during plasma process, and these groups are responsible for improving surface wettability, which is shown to correlate with improved cell growth since hydrophilicity of surfaces is preferable for protein deposition[30].

In this project, I studied the suppression of development of disordered structures for PDMS treated by oxygen plasma, by means of a simple prepatterning step. By combining the prepatterning process with plasma treatment, a new way to produce

ordered hierarchical structure was introduced. Surface morphology of such samples was systematically analyzed, and some biological applications have been demonstrated.

1.2 Scope of the present study

This thesis makes an attempt on showing the effect of prepatterns on suppressing or even guiding the development of ripples on plasma-treated PDMS surfaces, and investigating the effect of such surfaces on cell growth. Nano-imprint lithography was used to transfer prepatterns onto PDMS surfaces. The correlations between the geometries of the spontaneous patterns with different surface treatment conditions, such as plasma bias voltage and processing time, as well as the effect of surface prepatterns, were studied. During the period of this project, the fabricated surfaces were tested for cell culture studies with different cell types.

The thesis is arranged in the following way:

In Chapter 2, I give an overview of PDMS materials for nanosystems or biomedical applications. After a brief introduction, I review the surface modification technique used in this thesis work, namely plasma ion implantation and deposition. Then, I present the effects of plasma treatment on polymer properties, especially for the change of surface morphology. Finally, I review cell culturing experiments on plasma-

modified surfaces with topographic pattern. These include the basic concepts that are required to study the relationship between cells and substrates on which cells grow, (cells and cellular environment, polymer substratum for cell *in vitro* studies). Apart from this, I present the fundamental aspects of cell growth on the topographical patterns. Afterward, I present a literature review on the cell culturing of plasma-modified polymer surfaces.

In Chapter 3, an overview on the experimental methods is provided, including PDMS polymer preparation, the process for pattern transfer onto PDMS surfaces, equipment used for plasma treatment process, surface characterization techniques used in the project, as well as cell culture culturing process and characterization techniques.

Chapter 4 describes the experimental details and results of plasma treatment on PDMS samples. The correlations between spontaneous patterns with different surface treatment conditions, such as plasma bias voltage and processing time, as well as the effect of surface prepatterns, are also reported.

Chapter 5 focuses on the results of cell culturing on plasma-modified samples. A systematic cell culturing investigation on the topographic surfaces was conducted. By using MC3T3-E1 cells cultured on prepatterned samples, I demonstrated the importance of controlling the surface feature size of depth of prepatterning features on the cell

growth. In addition, HeLa cells were cultured on hierarchal pattern formed by high-voltage bombardment on prepatterned surfaces, and the influences on cell growth are reported.

Finally, I summarize the work and suggest some possible future activities in Chapter 6.

Chapter 2. LITERATURE REVIEW

As mentioned in Chapter 1, PDMS is a desirable material for industrial and biomedical applications; so, the chemical structure and properties of PDMS are reviewed at the beginning of this Chapter. Surface modification techniques are then introduced, especially for plasma ion implantation and the effect of plasma treatment on the changes of properties in polymer. Finally, cell culturing techniques are introduced, including the basic concepts that are necessary for studying the interactions between the cells and the culturing substrates. Some aspects of cell responses to patterned substrates and on modified polymer surfaces are summarized.

2.1 Polydimethylsiloxane

2.1.1 Introduction

PDMS is a silicone-based organic polymer which is widely used in industrial and biomedical applications, such as microfluidic devices [19], stamping [31] or biomaterials [32][33]. The most commonly-used commercial kit of PDMS is Dow Corning Sylgard Elastomer 184. This kit consists of two parts: a pre-polymer (base) and a cross-linker (curing agent). The mostly commonly used PDMS in research has the

pre-polymer and the cross-linker mixed in 10:1 weight ratio,. Different pre-polymer/curing agent ratios lead to different amounts of cross-linking [32]. When the two parts are mixed together, a crosslinking reaction cures the product into PDMS. PDMS consists of the repeated units of $[SiO(CH_3)_2]$ (Fig. 2.1). In the figure, *n* is the number of repeating units. Non cross-linked PDMS could be in liquid or semi-solid form, depending on the value of *n*. The siloxane bonds enable a flexible polymer chain, and since chain-to-chain interactions are low, a highly viscoelastic property can be obtained [34]. After the cross-linking process, PDMS achieves hydrophobicity, meaning that it is difficult to wet the PDMS using polar solvents such as H_2O.

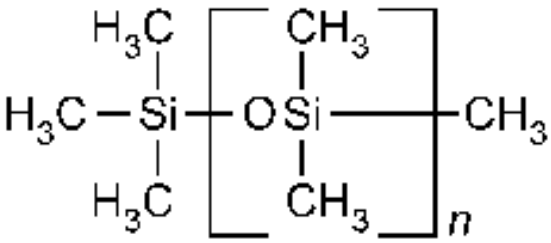

Fig. 2.1 Chemical structure of PDMS.

The practicability of polymers being manufactured by stamping or in mass production, as well as their low costs relative to silicon, make them attractive for various applications. Some of the commonly-used polymers include polycarbonate (PC),

PDMS, PMMA and polystyrene (PS) [4][5]. Among these, PDMS has attracted much attention in biomedical applications or nanosystems, for a number of reasons:

1. Features reproducible with high fidelity: PDMS can be molded with a resolution down to tens of nanometers [35].
2. Low cost: compared with other materials such as silicon, PDMS is cheap for chemical or physical modifications applications compared to other materials [36].
3. Low material processing loss.
4. High thermal stability and chemical inertness.
5. Simplicity in handling and manufacturing.
6. High permeability to gases, absence of toxicity, and excellent resistance to degradation which are attractive for cellular applications. For example, PDMS can be used for biomaterial implants for soft tissue augmentation, ear and nose implants, and other medical supplies such as drainage tubing materials, catheters, and insulation for pacemakers [37][38].
7. It is highly transparent from 240 nm to 1100 nm with low auto-fluorescence [39], so a lot of optical detection plans can be used. In contrast, other polymers have

unsaturated bonds or heteroatoms embedded in them, and they tend to absorb UV radiation and fluoresce substantially, causing problems for optical detection.

2.1.2 PDMS for biomedical applications and nanosystems

Recent advances in nanosystems technology provide new opportunities in the fields of biological and medical applications [40][41][42]. Micro-fabrication or micromachining methods offer the potential to handle biological problems at the dimensions of cells [43].

Features with nanoscale or micrometer-sizes can be fabricated from materials such as PMMA, polyethylene (PE) and silicon. The main drawbacks for using these materials in biomedical applications can be briefly stated in the following:

- Silicon-based micro-fabrication can be successfully made through photolithography. However, such devices are limited to planar structures, complex and expensive for fabrication, and require access to clean room facilities.
- Fabrication with other polymers can be more challenging than with PDMS. With thermoplastics, for example, there are difficulties associated with the molding process, which require stamping or embossing with uniform pressure at elevated temperatures. The control on temperature and pressure is crucial, such that the thermoplastic is soft

enough to be molded, but not to flow back into the channels of the mold. On the other hand, PDMS can be molded into various shapes during the curing process, which is convenient and does not require any sophisticated processing techniques.

- For biomedical implants, quality control of polymers must be stringent, and it is very important that the polymer properties do not vary from batch to batch. For other types of polymeric materials such as PMMA, polycarbonate, polystyrene, poly-olefins, there can be so much variability in polymer properties such that it is difficult to achieve reproducibility from chip to chip that are required by industrial standards [44].
- These characteristics make PDMS an excellent material for nanosystems and biomedical applications. In my research, the PDMS samples need to be treated by oxygen plasma. When freshly plasma oxidized, PDMS can be sealed to itself and to other materials without using any adhesive. Most of other polymers require adhesive for the sealing processes [44].

2.2 Surface modification of polymers

Although polymers possess unique properties, the inert nature of most polymeric materials creates challenges in various applications that demand specific surface properties, which are required for inking and printing processes, as well as wetting and

adhesion for coatings and biomaterials. For example, it is hard to introduce solutions into PDMS-based devices such as microfluidics due to their intrinsic hydrophobicity. In addition, as the electro-osmotic mobility (μ_{eo}) of PDMS is usually unstable, hydrophobic analytes can be readily adsorbed onto PDMS surfaces that can interfere with the characterization process [19]. Hence, surface modification of PDMS samples is critical to inhibit non-specific adsorption of hydrophobic species, improving wettability and stabilizing and improving μ_{eo}.

There are many surface modification methods of polymeric materials, which can be divided into gas-phase processes and wet chemical methods.

- Gas-phase processes include plasma treatment [15][16][17], ultraviolet (UV) irradiation [45], chemical vapor deposition (CVD) [46] and sputter coating of metal compounds [47][48][49].
- Wet chemical methods: layer-by-layer (LBL) deposition [50], sol-gel coatings [51], silanization [52], and dynamic modification with surfactants and protein adsorption [53].
- Finally, gas-phase processes and wet chemical methods can also be combined [19].

Plasma treatment can offer the modification of specific surface properties of samples, while the intrinsic bulk properties of materials are retained [22]. For example, the biocompatibility of titanium and titanium alloys can be improved while the corresponding bulk material attributes (such as mechanical properties) remain unchanged [54]. In this project, I used oxygen plasma treatment to modify the polymeric materials surfaces. Some basic concepts of plasma treatment, and the advantages of this method, are introduced in the next section.

2.2.1 Plasma surface modification

The term plasma was firstly introduced by Tonks and Langmuir [55]. Plasma is a physical system which consists of neutrals, molecules, atoms, excited particles, ions, electrons, photons, or a mixture of these (quasi)particles. Plasma behaves like gases in many aspects and obeys the gas laws. Plasma can be induced by supplying high energy (thermal, electrical, or electromagnetic radiation) to a gas system. For technical applications, however, plasma is often induced by electrical discharges.

Plasma surface modification has unique advantages, such as low processing temperatures, and is a non-line-of-sight and dry process. It is thus suitable for the treatment of polymeric materials that usually requires low processing temperatures.

Furthermore, the non-line-of sight nature of the process makes it possible to treat biomedical components with complex geometries. Besides, a dry process is always preferred to suppress the contamination on sample surfaces. The effects of plasma ion implantation on the changes of polymer properties are introduced in the next section, using PDMS as a representative example.

2.2.2 The effect of PIII on the change of properties of polymer

Plasma surface modification employs gases such as oxygen, nitrogen and hydrogen, which dissociate and react with the substrate surfaces, creating chemical functional groups in the process. This method of surface treatment is by far the most commonly used method for PDMS surface modification [56][57][58][59].

Some ongoing and formidable challenges with the oxidation of PDMS by plasma immersion ion implantation (PIII) include the hydrophobicity recovery caused by the migration of uncured PDMS oligomers from the bulk to the surface, and the rearrangement of highly-mobile polymer chains featuring Si-OH bonds towards the bulk at room temperature [60][61][62]. These effects can be attributed to the low glass transition temperature of PDMS, which is in the order of -120ºC [63].

Vickers *et al.* [61] managed to retain the hydrophilicity of PDMS for prolonged duration by employing a solvent extraction sequence involving triethylamine, ethyl acetate and acetone, to remove the oligomers before oxidizing the PDMS surface in an air plasma. After storing in air for 7 days, the water contact angle (WCA) of PDMS samples oxidized with such an extraction process increased from 30° to 40°, while the oxidation of PDMS that did not perform the solvent extraction process showed a change of WCA from 58° to 110° after 7 days. This indicates that solvent extraction renders the plasma-oxidized PDMS more hydrophilic and stable. An alternative method to preserve hydrophilicity of sample surfaces after plasma oxidation was demonstrated by Ren *et al.*[64], who found that a stable μ_{eo} of $4x10^{4}$ cm^2/Vs [19] could be maintained for over 14 days by keeping the surface in contact with water. They also found that after 14 days of storage in air, the immersion of surface in NaOH for 3 hours reinstated the μ_{eo} back to $4x10^{4}cm^2/Vs$, implying that uncured PDMS oligomers are being removed or the -OH groups are being reoriented to the surface after exposure to a base solution.

Surface texturing of polymers can be produced through plasma treatment, and this surface texturing process can be used to vary the surface wettability, biocompatibility, optical property and frictional characteristics of a material [65][66]. PDMS is known to form ripples and textured surface patterns after plasma treatment. Some important

investigations on using PDMS as the samples highlight the features of these surface waves[26][27][67][68][69][70][71][72].

By putting PDMS samples to an oxygen plasma treatment, Bowden *et al.* [27] obtained periodic waves that were locally ordered in very short range, but disordered in long range. After that, they used bas-relief structures for generating oriented undulation patterns. Chua *et al.* [26] got similar experimental results. They both found that longer plasma treatment resulted in larger surface features. Evangelos *et al.* also produced spontaneously surface ripples in random orientations, with the periodicity in the sub-micron scales [73] . In addition, they extended their work towards the fabrication of oriented nano-features on PDMS samples by placing a mask on it during the plasma treatment process [74]. Ashkan *et al.* [75] used a multi-step plasma technique for controlling the wrinkling patterns formation process, and succeeded in obtaining one-dimensional, two-dimensional, and even hierarchical patterns. They suggested that the parameters (amplitude and wavelength) of the wrinkling features could be adjusted by varying the processing time and stretching force applied on the PDMS during the plasma treatment step.

2.3 Cell culture on surface modified samples

2.3.1 Cells and cellular environment

Cells are the basic units of life. The molecular structure of cells is extremely complicated, which evolves in response to the external chemo-mechanical environment [76]. Fig. 2.2 shows the schematic of typical organization of an eukaryotic cell, which includes a nucleus, Golgi complexes, mitochondria, cell membrane, etc. The aquatic solution, which exists around the nucleus and organelles, is the cytoplasma. The outermost membranes can effectively protect cells and can be used as barriers to outside environment, adjusting the flow of nutrition, energy and exchange of information during cell interactions.

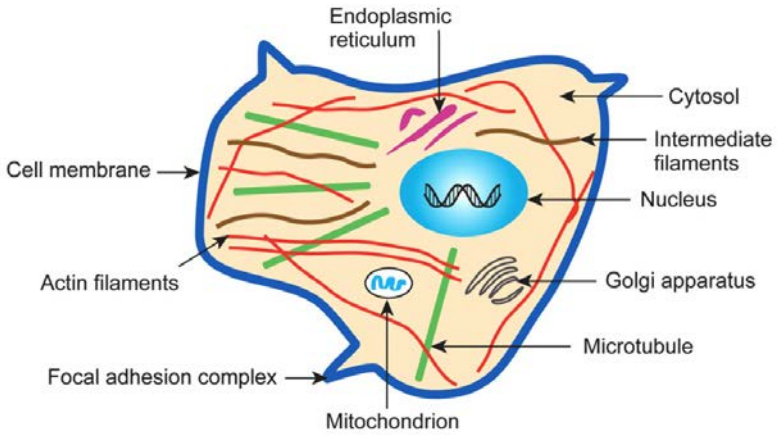

Fig. 2.2 A schematic of the typical microstructure of an eukaryotic cell [77]

Cytoskeleton is a filamentary network comprised of different types of multi-molecular polymers. The cytoskeleton acts not only as the structural element, but also contributes to the signal transduction between cellular interactions. The main filaments in these multimolecular polymers are: actin filaments, intermediate filaments and microtubes [78]. As shown in Fig. 2.3, unlike engineering polymer networks, a cytoskeleton is a highly dynamic structure of cross-linked proteins, with the on-off kinetic function to keep the filaments within themselves at the polymerization to de-polymerization state.

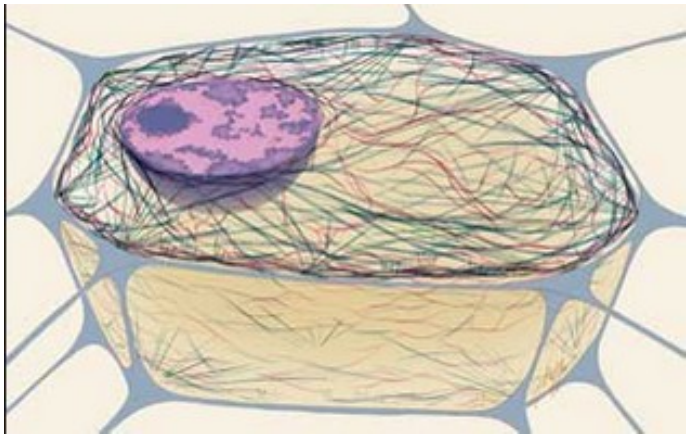

Fig.2.3 A typical scheme of cytoskeletal filaments in an eukaryotic cell [79].

In the cell environment, cells are brought together for forming a tissue through the help of an extracellular matrix (ECM). The extracellular matrix (ECM) consists of different molecules, which includes proteoglycan complexes, collagens, elastic fibers, etc. It plays an important role in maintaining tissue function and structure in a three dimensional manner, as shown in Fig. 2.4.

The extracellular matrix (ECM) is an important bridge for passing on the biochemical signals from tissues to the cell. The extracellular matrix is the connective tissue in animals, which consist of a complex mixture of functional and structural macromolecules arranged in a three dimensional manner. This cellular environment provides mechanical and biochemical signals to the cells [80]. Cells can feel the

mechanical stress stimulation from the ECM [81].The composition of ECM can affect matrix stiffness, nutrition-diffusion to tissues and cell-matrix interactions. Most cells require attachment to solid surfaces for cell growth and ultimately forming tissues or organisms [82], because tissue formation are defined by cycles of mechanical sensing, mechanical transduction and mechanical response which are from local sensing of force or geometric features on the substrate. These local sensing will be transduced into biochemical signals to affect cell adhesion, cell morphology, cell proliferation, cell differentiation and cell death. In tissue engineering, there is a viewpoint that cell adhesion precedes any other cell behaviors [83]. Hence, a hot topic in biomaterial research field is to analyze the relationship, such as response mechanism between adhering substrate and cells [84].

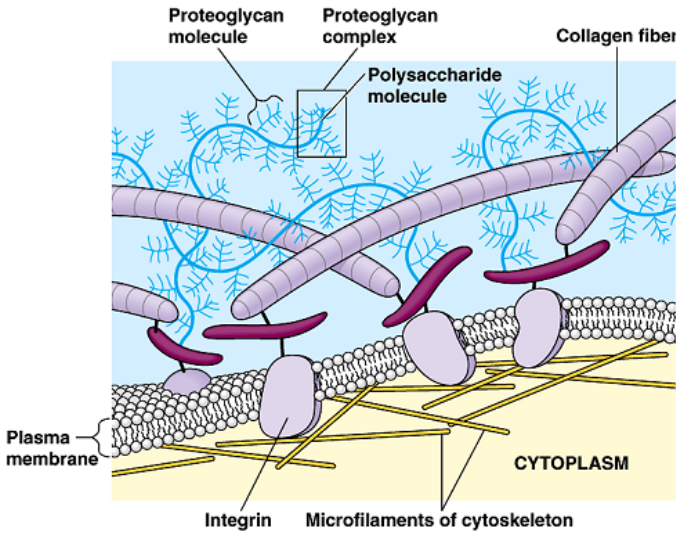

Fig. 2.4 A schematic picture of extracellular matrix (ECM) [66].

2.3.2 Polymer substrates for *in vitro* cell studies

Synthetic polymers are important candidates for biomaterials and engineering tissues [85]. Several classes of polymeric materials have proved to be useful in biomedical applications, which include cases where polymers remain in intimate contact with the cell and tissues for a long time. Examples of some polymers used as biomaterials are listed in Table 2.1.

Table 2.1 Examples of different polymers used for biomedical applications [86].

Polymer	*Medical applications*
Polydimethylsiloxane, silicone elastomers (PDMS)	Breast, penile, and testicular prostheses
	Catheters
	Drug delivery devices
	Heart valves
	Hydrocephalus shunts
	Membrane oxygenators
Polyurethanes (PEU)	Artificial hearts and ventricular assist devices
	Catheters
	Pacemaker leads
Poly(tetrafluoroethylene) (PTFE)	Heart valves
	Vascular grafts
	Facial prostheses
	Hydrocephalus shunts
	Membrane oxygenators
	Catheters
	Sutures
Polyethylene (PE)	Hip prostheses
	Catheters
Polysulphone (PSu)	Heart valves
	Penile prostheses
Poly(ethylene terephthalate) (PET)	Vascular grafts
	Surgical grafts and sutures
Poly(methyl methacrylate) (pMMA)	Fracture fixation
	Intraocular lenses
	Dentures
Poly(2-hydroxyethylmethacrylate) (pHEMA)	Contact lenses
	Catheters
Polyacrylonitrile (PAN)	Dialysis membranes
Polyamides	Dialysis membranes
	Sutures
Polypropylene (PP)	Plasmapheresis membranes
	Sutures
Poly(vinyl chloride) (PVC)	Plasmapheresis membranes
	Blood bags
Poly(ethylene-*co*-vinyl acetate)	Drug delivery devices
Poly(L-lactic acid), Poly(glycolic acid), and Poly(lactide-*co*-glycolide) (PLA, PGA, and PLGA)	Drug delivery devices
	Sutures
Polystyrene (PS)	Tissue culture flasks
Poly(vinyl pyrrolidone) (PVP)	Blood subsititutes

By selectively modifying surface properties of the polymer, such as surface topography or roughness, distribution of chemical groups, and hydrophilic/ hydrophobic properties, polymeric substrates should not only stimulate the cell adhesion and proliferation, but also the formation of ECM and tissue regeneration [87].

There is a lot of room for enhancement in polymeric materials for biomedical applications and tissue engineering, due to the short development history and increasing demands for various medical procedures. In order to meet the demand for improved biomaterials in the field of tissue engineering, polymeric biomedical materials which interface well with living tissues and possess good biocompatibilities, are required.

2.3.3 Cellular responses to topographic patterns

The ability to modify sample surfaces with regular patterns and chemical clues, by means of lithography or nanoimprinting processes, is critical to control the cell growth such as cell behavior, cell proliferation and cell differentiation. Micro-fabrication techniques [88] prepare features in the micrometer scale on the sample surfaces, which is of the same dimension as the ECM. The substrate-cell interaction can be directly probed, and cellular behavior could be observed through microscopes.

In the past few years, many researches were conducted about the surface micro-texturing effect on cellular behavior, cell elongation and cell growth direction. For instance, Rovensky *et al.* utilized V-shaped grooves to stimulate chick embryo fibroblasts movement [89]. They found that after a few hours, the chick embryo fibroblasts moved from the bottom of grooves to the top surface, and aligned along groove directions. The response of cells to substrate topography is termed "contact guidance" [90]. Weiss *et al.* assumed that fibrils oriented by tension in a particular direction, which would affect the cells to align the same orientation. Fig. 2.5 shows a comparison of epithelial cells, which align well on a structured substrate, but otherwise spread into a circular shape on a smooth surface [91].

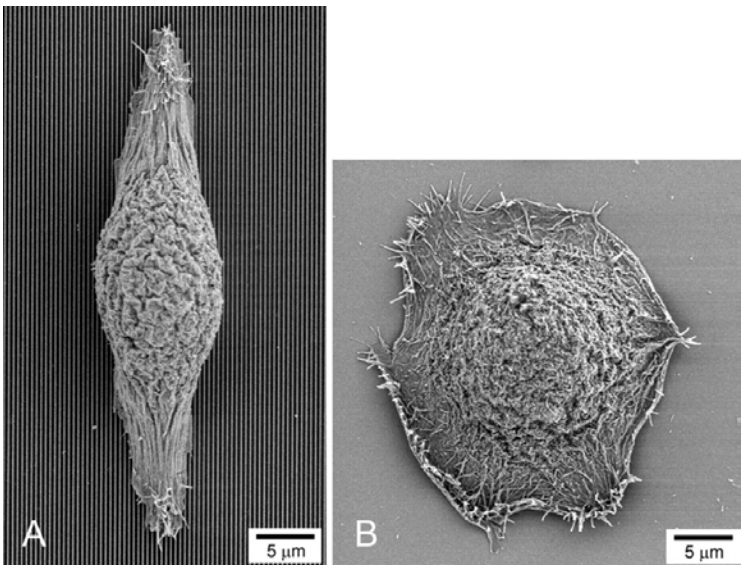

Fig. 2.5 Images of human corneal epithelial cells. (A) Cell cultured on patterned silicon dioxide surface; (B) Cell cultured on a smooth silicon dioxide surface [91].

Den Braber conducted experiments to study rat fibroblast cell behavior on control flat silicon surfaces and microtextured silicon wafers. The grooves were of different sizes (width from 0.45 to 10 μm and depth of 0.5 μm [92] [93] [94] [95]). The results revealed that on grooves with width less than 4 μm, the cells were strongly elongated and aligned to the direction of grooves. When the groove width was larger than 4 μm, the cell oriented randomly. They deduced that the groove width was a more critical factor to affect the cell alignment than the groove depths [93]. Walboomers and Alaerts *et al*. also obtained similar results. They found that on grooves of widths 5 and 10 μm, the cells adhered within the grooves. On narrower grooves of widths 0.5, 1 and 2 μm, cells were elongated and aligned along the grooves, with each cell covering several grooves [96][97].

Researchers have suggested some possible mechanisms behind the phenomena of contact guidance. For instance, Lenhert *et al*. [98] suggested that contact guidance was induced by the capillary force exerted by the parallel grooves. Dalby et al. [99] found that grooves might deform the nucleus in the cells and changed the gene expression, which caused the cells to align. Zhou et al. [100] revealed a relationship between the cell membrane deformation and cell alignment by using reverse cellular printing.

In my project, the observations on cell alignment were not only made on the prepatterned PDMS surfaces, but also on plasma-modified prepattened PDMS surfaces. In addition, cell adhesion and cell proliferation tests were also investigated. It was hoped that as more investigations were conducted, a better understanding of cell behaviors involved could be achieved, and the importance of surface modification of polymers in biomedical applications could then be revealed.

2.3.4 Cell culturing on plasma modified polymer surface

Plasma surface modification is commonly used to modify polymer surfaces. Plasma ion implantation can strongly optimize surface properties of polymers, such as surface biocompatibility and bio-functionality, while the favorable bulk characteristics, such as strength and inertness, can be retained [101]. Plasma modification can also significantly change the hydrophilicity, refractive index and hardness of polymers [22]. New functional groups [102] can be implanted to the surface materials through the use of specific gases for reactions. For example, amino groups can be added to the polymer surface in a nitrogen plasma reaction system. On the other hand, it is difficult to exactly determine the effect of plasma surface modification, since plasma reaction is a very

complex process, and plasma-treated layer thickness is typically of only tens of nanometers. Some examples are listed below.

The surface hydrophilicity of chitosan membranes can be increased through an argon plasma treatment, which promotes the adhesion and proliferation of human-skin-derived fibroblasts cultured on them [103]. Kwok *et al*. reported plasma immersion ion implantation of PC and polytetrafluoroethylene (PTFE) using argon and oxygen, respectively, with different process parameters such as pulse width and frequency. High-energy oxygen treatment resulted in a super-hydrophobic PTFE surface that was characterized by a higher affinity for human cells [104]. Acetylene (C_2H_2) plasma ion implantation treatment of polyethylene terephthalate increased the hemocompatibility and antibacterial properties of the materials, with a significant decrease in bacteria adhesion and growth [105]. The changes in wettability, chemical properties and texture of PMMA surface through air plasma treatment can promote the adsorption of Bovine Serum Albumin (BSA) onto treated samples, which may be beneficial to cell attachment on biopolymer surfaces [106].

2.4 Summary

In summary, PDMS possesses unique properties that can be applied in microfluidics and cell culture studies. PDMS shows some characteristics, such as high permeability to gases, reproducible features with high fidelity, and absence of toxicity. Plasma surface modification can selectively optimize surface properties of polymers while bulk attributes can be maintained well. This surface modification method, and the effect of plasma treatment on the surface property changes of PDMS, were reviewed. The basic background of cell culture study was introduced. The types of polymeric materials can be used as bio-substrates for cell culture were listed. The response of cells to patterned substrates and plasma modified polymer surfaces were also summarized. By seeding cells on different materials and in various patterns, this method could be used for guiding cells in a special direction or adapting specific function [107]. The charge distribution changes and surface oxidation improvement of polycaprolactone films after plasma treatment, resulted in promoting human renal epithelial cells attachment and proliferation [108].

Chapter 3. EXPERIMENTAL METHODS

In this Chapter, the fabrication of prepatterned PDMS samples and the plasma implantation treatment method are introduced. The method of culturing cells on PDMS is also explained. Sample characterization methods, including atomic force microscopy and scanning electron microscopy, were used in this project to observe the surface morphology and cell growth on PDMS surfaces. Basic principles of these techniques are briefly explained.

3.1 Materials preparation

3.1.1 Fabrication the PDMS prepatterns

Fig. 3.1 illustrates the process flow of PDMS pattern generation. Elastomeric PDMS (Sylgard 184, Dow Corning) was prepared by mixing the siloxane base and curing agent in a weight ratio of 10:1. The mixture was cast onto polycarbonate master molds with grating tracks of two different dimensions: (1) periodicity of 1.5 μm and depth of 150 nm, and (2) periodicity of 0.75 μm and depth of 100 nm. Control samples with flat surfaces were made, by casting PDMS on cleaned glass slides. Subsequently the mixture was degassed by placing the sample in a vacuum until all the bubbles were

taken away, and the samples were then cured at 75ºC for 1 hour.

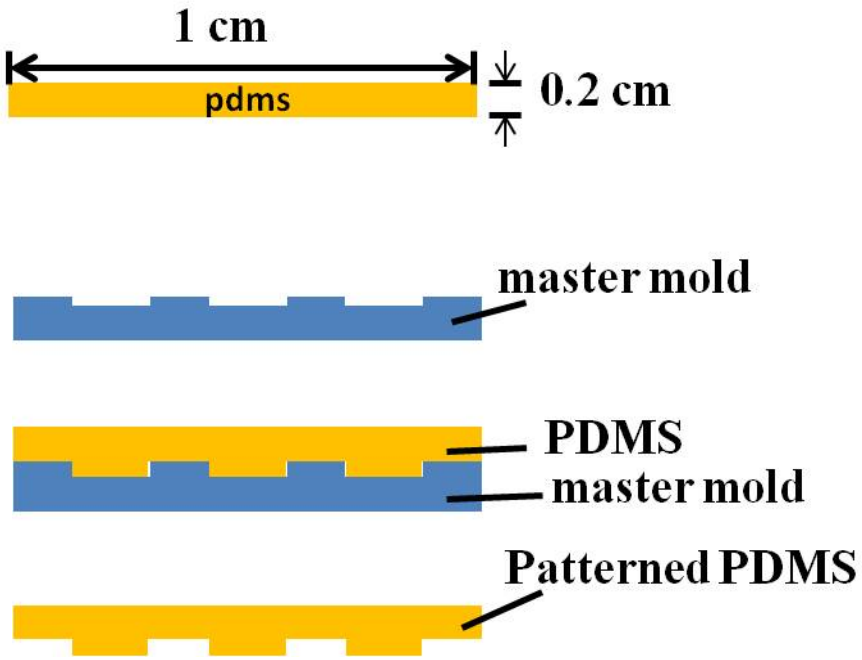

Fig. 3.1 Process flow of PDMS pattern generation.

3.1.2 Plasma implantation treatment

Fig. 3.2 depicts the oxygen plasma ion implantation setup. The setup comprises three main parts: (1) plasma implantation chamber, (2) pumping system, and (3) high voltage power resource. The plasma ion implantation system consists of a stainless steel cylindrical chamber (ø 760 mm × 1030 mm) with a rectangular front door. This chamber was used for modifying PDMS samples in this work. The plasma is generated by a radio frequency (RF) discharge of 13.56 MHz with an averaged power of 1 kW.

In the ion-implantation system, the control and prepatterned samples were

placed side-by-side on the sample stage. The sample stage was connected to the negative electrode of a high bias voltage power source. Oxygen or other gases can be fed into the chamber through the flow controllers and inlets of the implantation chamber. The samples were connected to a high negative potential (0 kV to 40 kV relative to the chamber wall), and the positively-charged ions in the oxygen plasma were accelerated across the sheath formed around the samples and implanted into the sample surface. If the applied voltage pulse were long, it would allow a plasma sheath to expand to the chamber wall, causing instability and finally plasma extinction [109]. In the specific direct-current (dc) plasma setup used in this project, a grounded conducting grid was used for blocking ion sheath expansion, and then a continuous low-pressure discharge was maintained in the plasma production region. In the plasma implantation region, a strong electric field was created between the grid and negatively-biased sample stage [110]**.** The grid separated the vacuum into a plasma production region and a plasma implantation zone. This kind of quasi-dc plasma setup retains the pulsing characteristics but prolongs the duration of applied voltage pulse without extinction of plasma. This technique also prevents the accumulation of charges on the sample surfaces and minimizes the sample overheating [111]. The technique is a non-line-of-sight process and has advantages compared with conventional beam-line plasma

ion implantation [112]. The base pressure in the implantation chamber was 2.4×10^{-3} Pa [113]. The oxygen pressure was maintained at 0.1 Pa during the plasma treatment process, with a flow rate of 10 sccm. In this work, I adopted a long-pulse, high frequency quasi-dc oxygen plasma ion implantation procedure. The sample voltage pulse width was 50 μs and the frequency was 100 Hz. Detailed experimental parameters are discussed in Chapter 4.

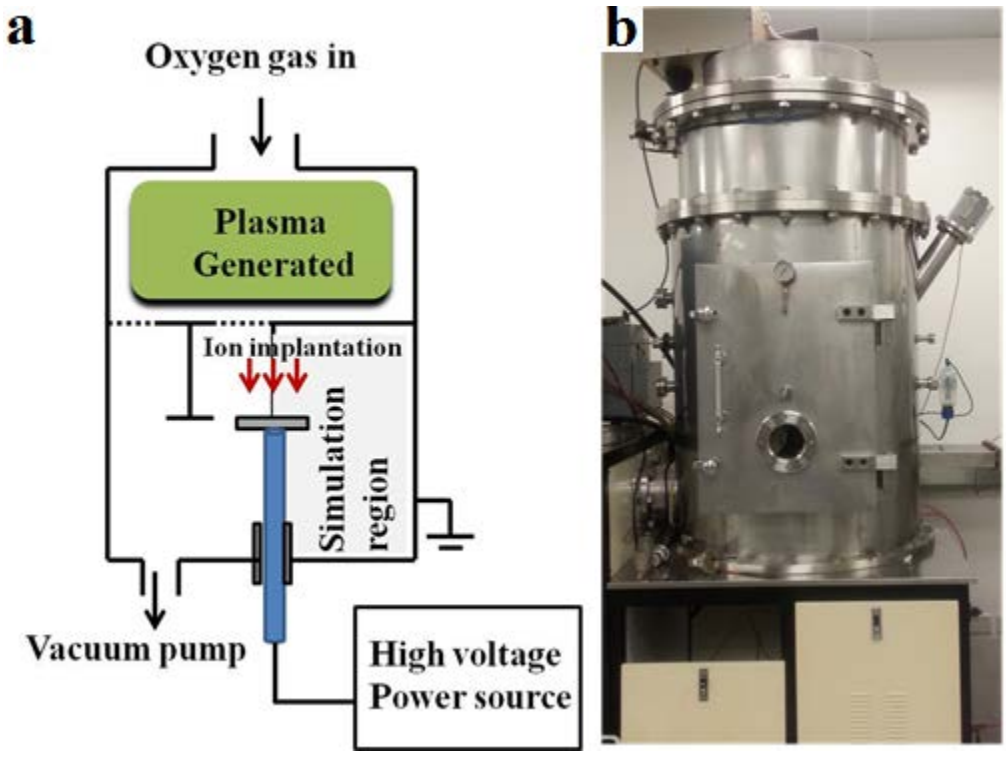

Fig. 3.2 (a) Schematic diagram of direct-current plasma implantation setup. (b) The dc plasma implantation chamber used in this project.

3.1.3 Atomic force microscopy

Atomic force microscopy (AFM) was used to characterize the morphology of the PDMS patterns. An AFM setup consists of a cantilever, a photodiode, a laser source and controller electronics such as a piezoelectric scanner. The working principle of AFM is shown in Fig. 3.3. The cantilever is typically made of Si or Si_3N_4, and the tip has a radius of curvature around 10 nm. When the tip approaches the sample surface, the force between the sample and the tip results in a deflection to the cantilever. Typically, the deflection is amplified and measured by using a laser spot reflected from the top of the cantilever to the detector, and a feedback mechanism is used to regulate the tip-to-sample distance, thus maintaining a constant force between the sample and the tip.

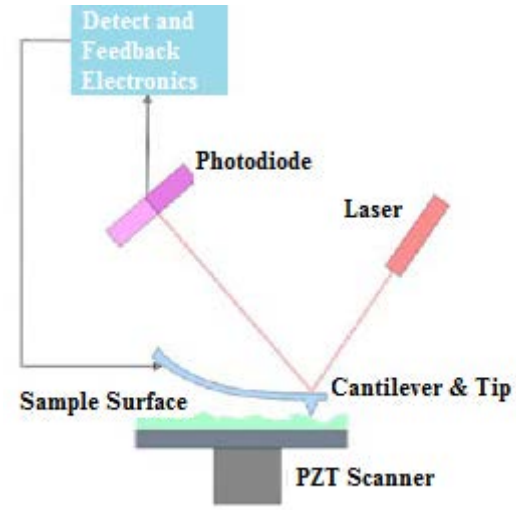

(a)

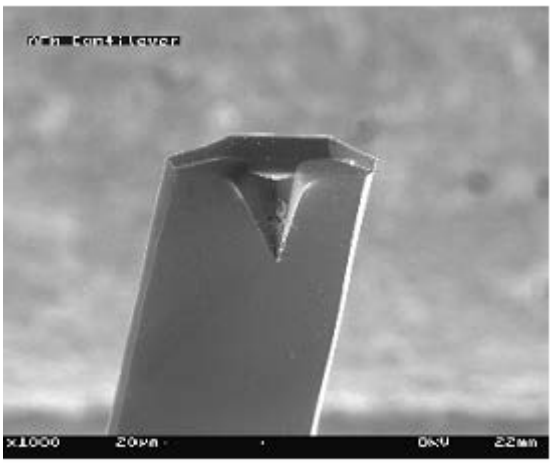

(b)

Fig. 3.3 (a) Working principle of AFM [114]and (b) an AFM cantilever[115].

During the AFM operation, the tip can either be in direct contact with the surface (Contact Mode), or simply tapped on the sample surface (Tapping Mode) [116]. Contact Mode operation can have issues of sample scratching and contamination. When the AFM tip scans on the sample surface, the computer records the interacting force

between the surface and the tip. This force is very sensitive to any environmental condition changes such as temperature, surface chemistry, humidity and mechanical and electrical noises. Tapping Mode is the preferred mode of operation, as the tip does not scratch the sample surface, so the surface features will not be destroyed [117]. In the Tapping Mode, an alternating voltage is connected to the piezoelectric scanner. When the tip reaches around its resonant frequency, it starts to scan over the sample surface. The sample stage changes its position to maintain the amplitude between the tip and the sample. This change of distance between the tip and sample induces the frequency change to the cantilever. These signals are converted into graphical images, which represent the sample morphology [118][119].

The AFM (Digital Instruments NanoScope 4 and 8) as shown in Fig. 3.4 were used in this project. The maximum sample size allowed was 10 x10 mm^2, and the surface roughness that can be measured was limited to 5 μm. During scanning, the sample moved in X and Y directions.

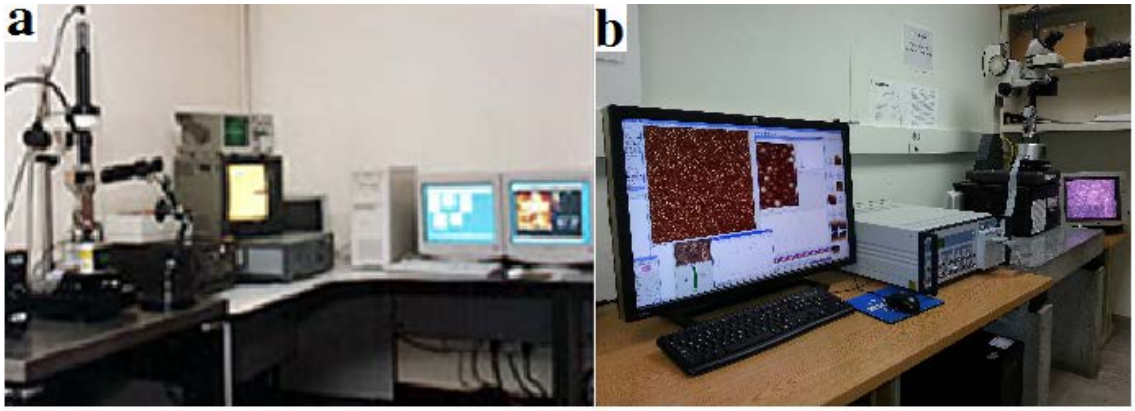

Fig. 3.4 Atomic force microscope (Digital Instruments NanoScope 4 (a) and 8 (b)).

3.2 Cell culture study and characterization

3.2.1 Cell culturing

To demonstrate the application of prepatterned PDMS samples or ion-implanted PDMS surfaces, the samples were used as substrates for cell culturing with different types of cells. To illustrate the biocompatibility of untreated and treated samples, cell proliferation and cell adhesion experiments were performed using the bone-forming cells of MC3T3-E1 Rat calvaria osteblasts and endothelial cells of EAhy926 at the City University of Hong Kong. In addition, cell alignment and cell elongation tests were conducted in the University of Hong Kong. A description of cell culturing on the sample surface is presented here, and the detailed experimental setups are discussed in Chapter 5.

Fig. 3.5 illustrates the cell culturing process. Cells were cultured in a humidified atmosphere environment (5% CO_2, 37℃) with a culture solution of Dulbecco's modified Eagle's medium (D-MEM, Invitrogen) supplemented with 10% newborn bovine serum (Hyclone) . After being expanded for an additional passage, the cells were dissociated with 0.05% Trypsin-EDTA solution at 37°C for 5 min. Then, the solution was neutralized by placing an additional medium in the culture dish. Afterwards, cells were re-suspended in the medium for seeding. Before seeding cells on the sample surface, all the samples were sterilized in 75% (v/v) ethanol for 45 minutes and rinsed three times with sterile phosphate buffered saline (PBS). In my experiment, approximately the same number of cells were cultured on the control samples and treated sample surfaces in 24-well tissue culture plates. After a fixed period, the samples were taken out to new 24-well tissue culture plates. The cells on the sample surface were released and counted. The cell morphology was observed by fluorescent microscopy or scanning electron microscopy.

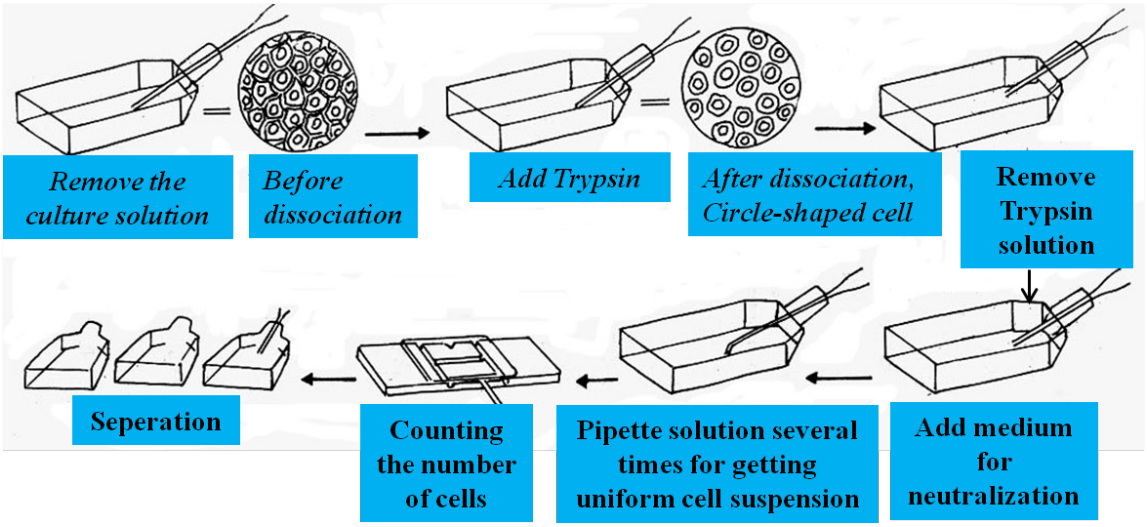

Fig. 3.5 Schematic diagram of cell culturing process [68].

3.2.2 Scanning electron microscopy

Scanning electron microscope (SEM) can image sample surfaces through scanning with an energetic electron beam and achieve high resolution. In this work, SEM was used to observe information of the cells.

Fig. 3.6 shows the working principle of a typical scanning electron microscope. A beam of electrons is emitted at the top part of the microscope from an electron gun. The electron beam passes a vertical path via the microscope in vacuum environment. The beam passes through electromagnetic condenser lenses, which is finally focused on the sample surface.

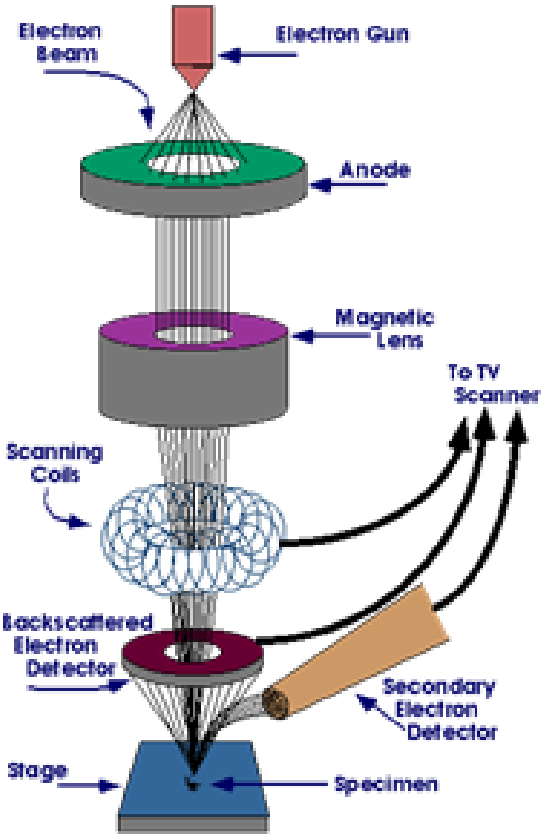

Fig. 3.6 Working principle of SEM [69].

When the incident electrons interact with the sample surface, different particles such as secondary electrons, backscattered electrons, Auger electrons, visible photons, X-ray and heat are produced as shown in Fig. 3.7 [120]. Secondary electrons from the top 5-10 nm of sample surface [120] and backscattered electrons contribute to the image formation in SEM [121].

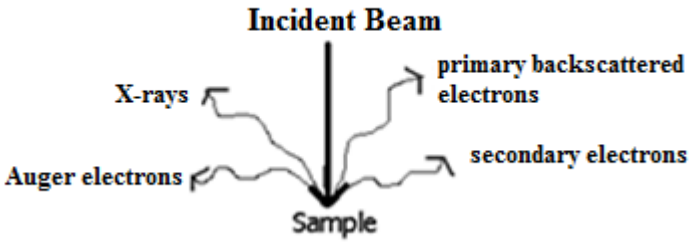

Fig. 3.7 Interactions between incident electrons with sample atoms [69].

Resolution is the critical factor for SEM characterization, instead of magnification. Higher resolution can be obtained by using higher accelerating voltages, shorter working distances, and larger apertures.

In this project, to test the compatibility and functionality of treated PDMS samples, high resolution images of cells on PDMS samples were obtained through SEM (Hitachi S-800) operating at 12 kV. Before being loaded into the SEM, the samples were fixed in a PBS solution containing 4 % formaldehyde for 30 minutes. Afterwards, the samples were rinsed twice using PBS, and immersed in 30% ethanol for 30 min. Then, the samples were dehydrated by using a graded series of ethanol solution and dried at nitrogen critical point. In the final step, a gold thin film of thickness 10 nm was deposited on the sample surface for preventing the charging effect of the samples.

3.3 Summary

To summarize, the prepatterning process was described and the modification of PDMS samples through plasma ion implantation was explained. Details of plasma ion implantation treatment were stated, including plasma ion implantation equipment, chamber environment and adjustable treatment parameters. For cell culturing, details of the cell culturing process were revealed. Pattern characterization techniques, including atomic force microscopy and cell morphology investigation using scanning electron microscopy, were introduced.

Chapter 4. WRINKLED PATTERNS STUDY

Wrinkling behavior on control flat surfaces and prepatterned surfaces is examined in this Chapter. Experimental details of plasma treatment are introduced, and surface morphology observation on prepatterns and flat surfaces treated by oxygen ion implantation are stated. Such morphology changes include the formation of wavy structures, the changes of prepatterned tracks, and surface-morphology variations between different initial surface morphologies. Last, I will discuss about the wrinkled pattern study in my project.

4.1 Introduction

Plasma ion implantation of PDMS can result in the formation of periodic structures in localized regions [26], the periodicity of which can be selected by controllable processing conditions such as bias voltage, processing time and prepatterning. The literature review on it has been done in Section 2.2.2

The aim of this part of project can be divided as follows. Firstly, the suppression on the development of spontaneously-induced wavy patterns during oxygen plasma process by employing prepatterns is studied. Besides, this prepatterning step can also be

used for controlling the development of the wrinkles with (sub) micron-micron scales, by varying the plasma treatment conditions and prepatterns, which can be used as molds for patterning of surfaces to transfer biological protein solution [28]. The relationship between surface features and the oxygen-plasma treatment conditions, such as bias voltage and duration time, is studied on flat surfaces of PDMS and prepatterned PDMS samples, respectively. This method opens up a possible way of generating oriented periodic structures on polymeric surfaces without utilizing non-lithographic techniques.

4.2 Experimental details

Table 4.1 depicts the oxygen plasma treatment details. After finishing the prepattern step mentioned in Chapter 3.1.1, tracks of period/heights 1.5 μm/140 nm and 0.75 μm/104 nm were successfully transferred onto PDMS samples. All the PDMS samples were cleaned in ultrasonic baths of ethanol and distilled water for at least 15 minutes each time before the plasma treatment. The samples (1 cm×1 cm) were put into the plasma chamber and subjected to oxygen plasma ion implantation. Table 4.1 shows instrument parameters during plasma treatment. The PDMS samples were subjected to oxygen plasma ion implantation with various bias voltages (0 to 10 kV) and processing times (15 or 30 min). The base pressure of the chamber was kept at 2.4×10^{-3} Pa. The

oxygen in the chamber was maintained at a pressure of around 0.1 and a flow rate of 10 sccm Pa during the plasma treatment. In this project, I applied a pulsed, high frequency quasi-dc plasma ion implantation procedure. Processing parameters are listed in Table 4.1. The bias voltage pulse width was 50 μs and the pulse frequency was 100 Hz.

Table 4.1 Instrument parameters used in PIII of the PDMS samples.

HV	RF				time	O_2
voltage kV	width μs	frequency Hz	power kW	frequency MHz	min	pressure pa
0	50	100	1	13.56	15	1
0	50	100	1	13.56	30	1
5	50	100	1	13.56	15	1
5	50	100	1	13.56	30	1
10	50	100	1	13.56	15	1
10	50	100	1	13.56	30	1

4.3 Surface morphology observations on prepatterns treated by plasma treatment

4.3.1 Effects of plasma ion implantation on the PDMS surface without geometry constrains

Fig. 4.1 illustrates the AFM micrographs of control (unpatterned) PDMS flat surfaces after treated by oxygen plasma ion implantation with different bias voltages

and processing time. Spontaneous formation of randomly-oriented ripple patterns can be found. Both the periodicities and the depths of the ripple patterns increased with rising bias voltage or processing time, but the patterns showed ordering only in localized regions. Besides, lots of cracks were generated on the surfaces, which significantly increased the surface roughness. It has been reported [26] that patterns occurred as the plasma treatment oxidized the PDMS surface to induce a silica-rich surface layer. During the oxygen plasma treatment, the PDMS samples expanded because of the rising temperature. When it cooled, the PDMS contracted much more than the silica-like surfaces because of its larger thermal expansion coefficient [122], which led to a large compressive stress in the top silica-like layer. A spontaneous surface buckling instability [123] was produced from releasing the compressive stress.

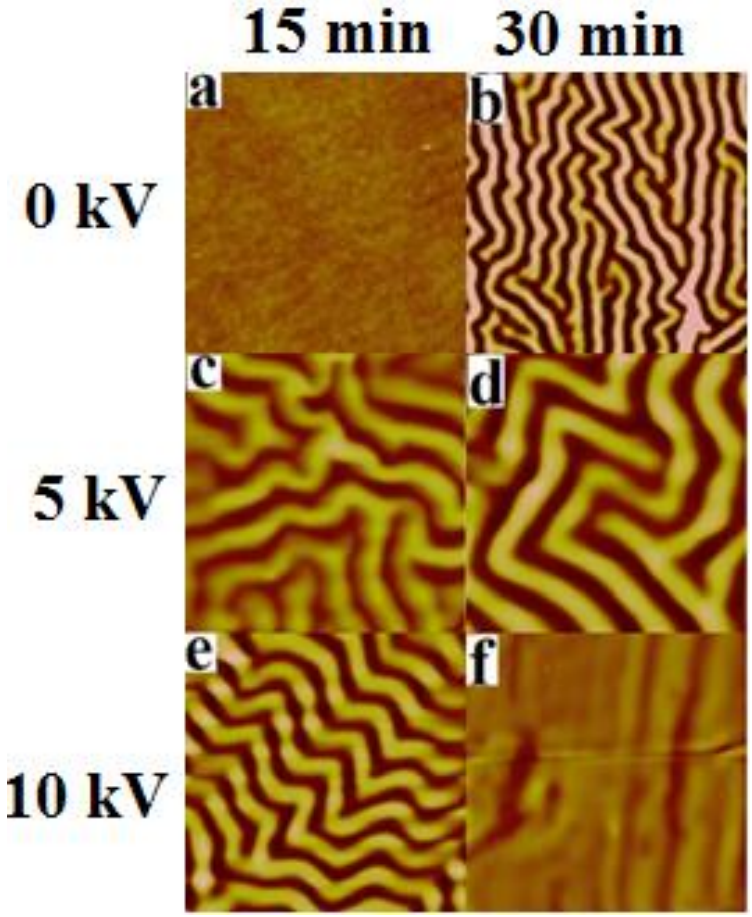

Fig. 4.1 AFM images of PDMS control flat surfaces after being subjected to oxygen ion implantation, with different processing times and bias voltages. (a) and (b): scan area = 10μm×10μm; z scale = 30 nm. (c) and (d): scan area = 10 μm×10 μm; z scale = 300 nm. (e) and (f): scan area = 60 μm×60 μm; z scale = 1000nm.

4.3.2 Effects of plasma treatment on the depth changes of prepatterned tracks

The change of depths (peak-to-trough distance) of the prepatterns on the PDMS samples, upon oxygen-ion bombardment, is shown in Fig. 4.2. Generally the prepatterns depth decreases with increasing bias voltage and processing durations, except for the 1.5 μm PDMS features implanted at 5 kV which showed an *increased* height variation This is repeatable in several samples fabrication under identical conditions. This special behavior, combined with the absence of randomly oriented ripple patterns on the PDMS surface (Fig. 4.3), can be explained by the increased compressive stress in the PDMS during the plasma process before it is released through ripple pattern formation.

Fig. 4.4 shows AFM images of PDMS samples with tracks of period (height) 0.75 μm (104 nm) after being exposed to oxygen plasma with different bias voltages and processing times. From Fig. 4.4 (a) and (b), the prepatterning features can be observed after being immersed in the oxygen plasma atmosphere for 15 min and 30 min, respectively. By applying a 5-kV bias to the sample during the plasma treatment, oriented sub-micron structures with periodicities are on the sample surfaces (Fig. 4.4 (c) and (d)). The periodicity, depth and regularity of oriented sub-micron structures increase

with rising bias voltages to 10 kV (Fig. 4.4 (e) and (f)). The spontaneous ripples are ordered on the PDMS surfaces, and the patterns showed high uniformity across the sample surface.

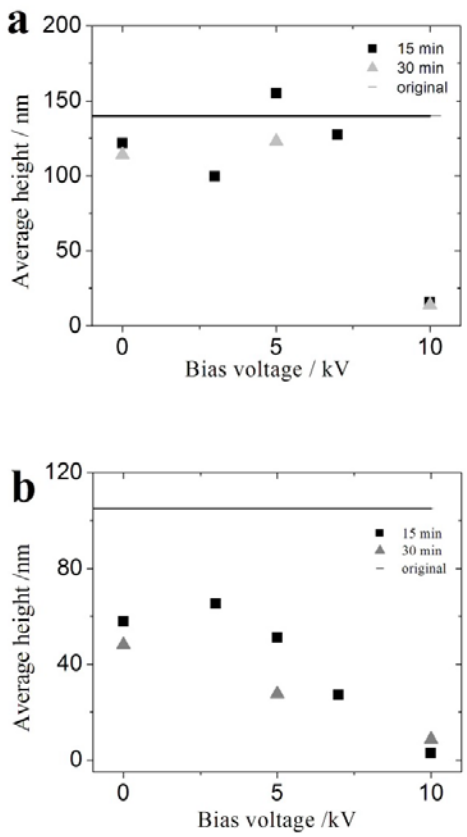

Fig. 4.2 Height variation for the original features on the pre-patterned PDMS samples under different bias voltages for different durations. Original patterns on the PDMS samples were tracks of period (heights) of 1.5 μm (140 nm) (a) and 0.75 μm (105 nm) (b). Original heights of the tracks are identified by the solid lines in the figure. Error bars for each data are smaller than the symbol sizes.

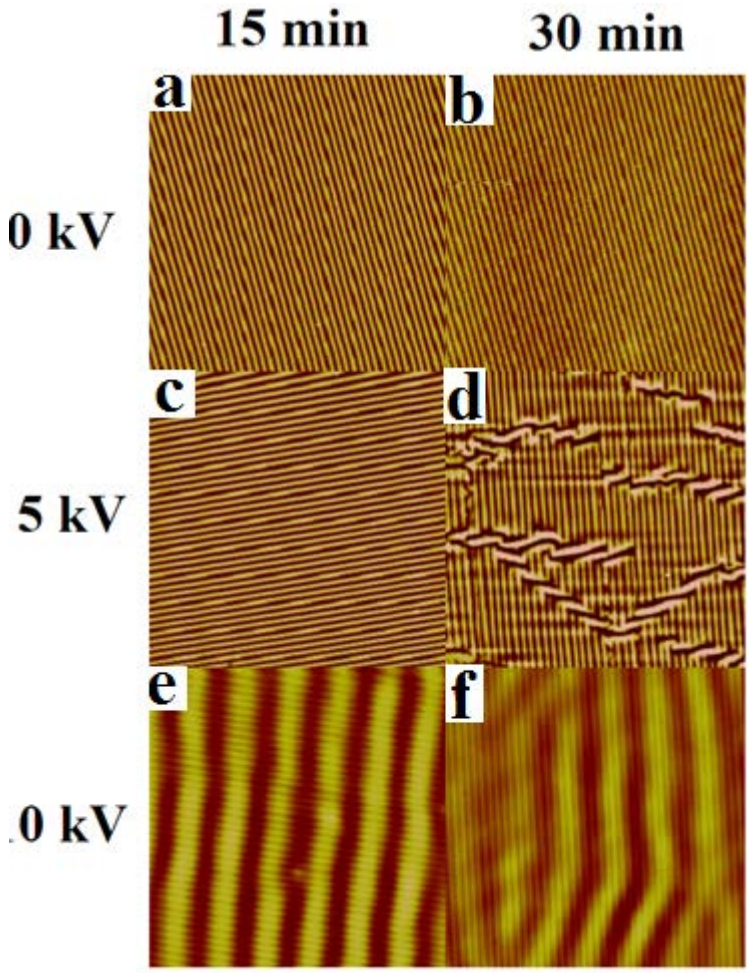

Fig. 4.3 AFM images corresponding to PDMS samples with tracks of period (height) 1.5 μm (140 nm) after being exposed to oxygen plasma treatment with different bias voltages and durations. All the scan areas are 60×60 μm^2 and z scale bar is 250 nm.

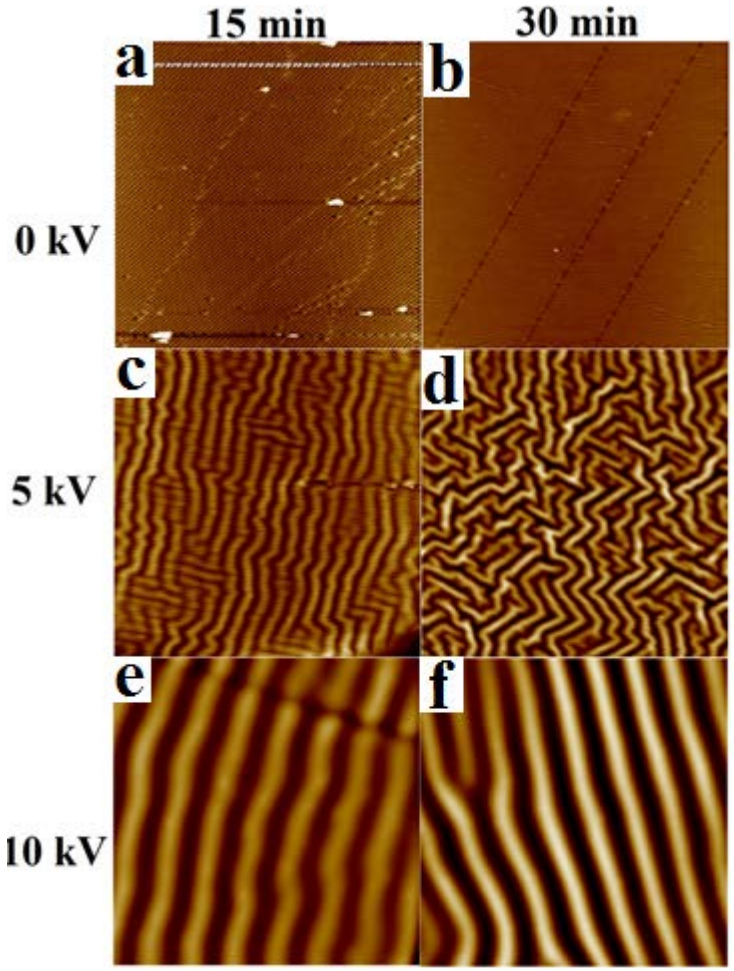

Fig. 4.4 AFM images corresponding to PDMS samples with tracks of period (height) 0.75 μm (104 nm) after exposed to oxygen plasma treatment with different bias voltage and duration. All the scan areas are 60×60μm and z range of images are 200 nm for (a) and (b), 600 nm for (c) (d) (e) and 800 nm for (f).

4.3.3 Effects of plasma treatment with different conditions on the morphology changes of prepatterns

➢ ***Tracks of period (heights) of 1.5 μm (140nm)***: Fig. 4.3 presents AFM images of prepatterned samples with tracks of period 1.5 μm and depth 140nm, after treated by oxygen ion implantation with different bias voltages and processing time. No undulation pattern was produced by the oxygen plasma treatment, when the prepatterns were exposed to a bias voltage of 5 kV, up to 30 min of duration time (Fig. 4.5 (a) and (b)). This is in strong contrast with the control flat PDMS samples, which show ripples even when subjected to oxygen plasma deposition without applied bias voltage (Fig. 4.2 (b)).

Besides, regular hierarchical structures were formed when the PDMS samples were treated by oxygen plasma with a bias voltage of 10 kV for 15 min, and the waves showed high uniformity across sample surfaces in a large area (Fig. 4.5 (c)). This is in contrast with the control flat surfaces samples (Fig. 4.2), which shows disordered ripple patterns. A regular compound pattern was observed in prepatterned surfaces, which resulted from the confinement and guidance from the surface features. The orientation of the ripples produced by plasma ion implantation was perpendicular to the prepatterns, hence the orientation of spontaneously ripple development can be well-controlled.

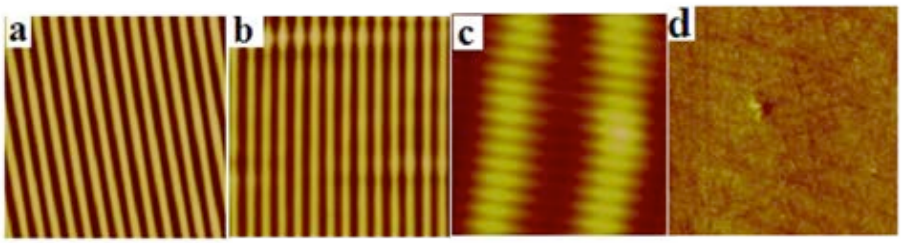

Fig. 4.5 AFM images of prepatterned PDMS samples (tracks of period (height) 1.5 μm (140 nm), after being subjected to oxygen plasma treatment with different bias voltages and processing times: (a) bias voltage of 5 kV for 15 min; (b) bias voltage of 5 kV for 30 min; (c) bias voltage of 10 kV for 15 min; (d) original PDMS flat surface without any treatment. Scan areas are all (20 μm×20 μm), and z ranges are 250 nm for (a) to (c), and 30 nm for (d).

- **Tracks of period (heights) 0.75 μm (105 nm):** Fig. 4.4 presents AFM images of prepatterned samples with tracks of period (height) 0.75 μm (105 nm), which were subjected to oxygen plasma treatment with different bias voltages and processing times. Spontaneous ripples can be found when prepatterned samples were implanted at the bias voltage of 5 kV for 15 min, up to 30 min implantation time. This is in contrast with the mentioned prepatterning samples (gratings of period 1.5 μm and depth 140 nm) (Fig. 4.4 (a) and (b)), which have shown no ripple patterns induced after identical plasma

treatments. However, when the sample was subjected to the plasma implantation of 10 kV for 15 min, the regular groove- patterns can be found across the large area (Fig. 4.6 (c)). This is in comparison with the control PDMS sample (Fig. 4.2 (e)), which showed irregular waves on the sample surface when the bias voltage of 10 kv was applied for 15 min. Although the prepattern (tracks of 0.75 μm and depth 105 nm) cannot be seen obviously as the sample in Fig. 4.3 (c), the tracks produced by plasma treatment are regularly oriented. The result may suggest that the controlled orientation of spontaneously pattern growth can be obtained through an appropriate combination of plasma treatment condition and prepatterning types.

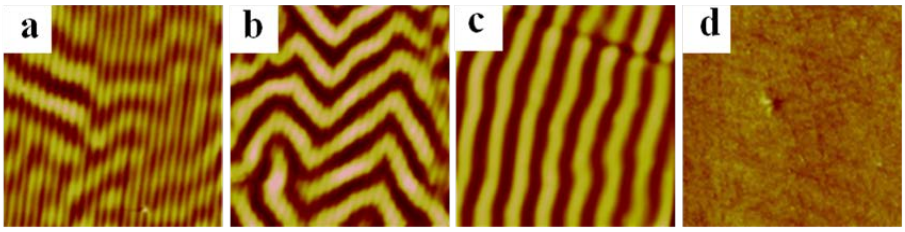

Fig. 4.6 AFM images of prepatterned PDMS samples with tracks of period (height) 0.75 μm (105 nm), after subjected to oxygen plasma treatment with different bias voltage and processing time: (a) bias voltage of 5 kV for 15 min; (b) bias voltage of 5 kV for 30 min; (c) bias voltage of 10 kV for 15 min; (d) original PDMS flat surfaces without any treatment. Scan areas of AFM images are (20 μm×20 μm) for (a), (b) (d) and (60 μm×60μm) for (c), and z ranges are 200nm for (a) (b)(c) and 15 nm for (d).

4.3.4 Comparison in surface-morphology changes between different initial surface morphologies after undergoing identical oxygen plasma treatment

Fig. 4.7 showed the AFM surface morphologies of three samples with different initial surface features but subjected to identical oxygen plasma treatment processes (10 kV bias for 15 min). Parameters of the produced wrinkle patterns are shown in Table 4.1. The periodicity of ordering spontaneous ripples was much larger on the

prepatterning surface when compared with the control flat surfaces samples; the peak-to-trough amplitude of ripple patterns on prepatterned samples was dramatically suppressed. This result suggests that the presence of initial surface features has suppressed the depth development of spontaneous ripple patterns.

The function of surface prepatterning in suppressing the development of high-roughness and irregular ripple patterns has been highlighted in many studies. Very often elastomer surfaces need to be plasma treated before they are used in different fields[13]. Unfortunately this would bring surface damages and irreversible changes to the sample morphologies, complicating the interpretation of experimental results. With the help of mild surface modulations (~ 105 nm height) it opens up a possible way to suppress the appearance of very severe surface roughness, which would be otherwise induced even in the absence of bias voltage during the plasma treatment process (Fig. 4.6). When wrinkles appeared on prepatterned samples at very high bias voltages, the surface amplitudes formed were much smaller if compared with the control samples (without prepatterning) (Table 4.2). Therefore we conclude that the surface prepatterning can provide a simple and effective method for suppressing the development of implantation-induced wrinkle patterns.

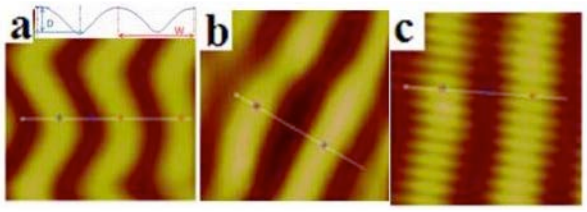

Fig. 4.7 AFM images of PDMS samples with different initial surface features (control flat surface (a), tracks of periods 0.75 μm (b) and 1.5 μm (c), respectively), after subjected to oxygen plasma treatment with bias voltage of 10 kV for 15 min. Scan area is (20 μm×20 μm) for all images and z range of the images are 1.5 μm for (a) and 250 nm for (b), (c).

Table 4.2 Parameters of surface modulations on control (flat surfaces) and prepatterned surfaces after treated by oxygen plasma ion implantation at bias voltage of 10 kV for 15 min. For prepatterned surfaces, compound structures were observed and the parameters for both pattern sets are illustrated.

sample	Main pattern		Secondary pattern	
	Periodicity (μm)	Depth (nm)	Periodicity (μm)	Depth (nm)
Control flat surface	6.35	704	-	-
0.75 μm tracks	8.25	187	0.745	2.75
1.5 μm tracks	9.68	127	1.42	14.32

4.3.5 Theoretical explanation of wrinkling pattern phenomena

We begin to consider wrinkling pattern of stiff sheets attached to the elastic foundations. If a compressive stress exerted on a skin-side of such a sandwich panel (eg.

a thin film resting on the top of an elastic foundation) exceeds the critical value, irreversible damage can occur on the sample surface and the construction may lose its own rigidity. A simple model has been employed in the past half a decade to demonstrate the principles leading to the formation of wrinkles [124][125][126][127][128]. In Figure 4.8, consider a thin film having a thickness h and width w, which is attached to a thick elastic foundation. Ignoring any shear stress between thin film and foundation and considering only the Poisson ratio and the elastic modulus of the thin film and foundation E_f, $V_{f,}$ and E_s, $V_{s,}$ respectively. The force can be given by the equation 1:

$$F = E_s\left[\left(\frac{\pi}{\lambda}\right)^2 \frac{wh^3}{3(1-v_s^2)} + \frac{\lambda}{\pi}\frac{E_f w}{4(1-v_f^2)E_s}\right] \qquad (1)$$

Buckling will happen in the thin film when exerted loadings exceed a certain critical value, F_c. Then the corresponding wavelength of the wrinkles is:

$$\lambda_c = 2\pi h\left[\frac{(1-v_f^2)E_s}{3(1-v_s^2)E_f}\right]^{1/3} \qquad (2)$$

From equation2, we can see that the wavelength of the ripples depends only on the material's own properties of thin film and foundation (their elastic modulus and their Poisson ratio) and thickness of thin film. It is independent of strain and applied force. The wrinkle wavelength is small for small (E_s/E_f) and h; it increases very significantly with increased both (E_s/E_f) and h [129]. In our experiment results, Table 4.2 shows the wrinkle period appeared on prepattened samples is much larger if compared with control samples after plasma treatment with same conditions, which means prepattern may contribute to the increase the thickness of thin film in the process

of plasma treatment.

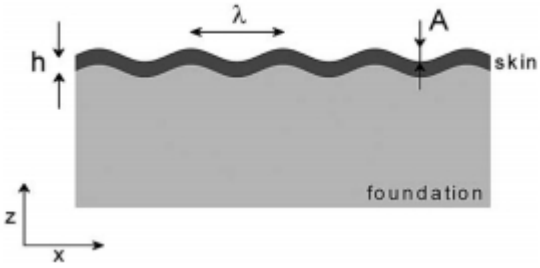

Fig. 4.8 The schematic of the geometry of wrinkles on a thin skin resting on the top of a thick elastic foundation, the skin has a thickness h and the wrinkles have the periodicity of λ and amplitude of A [129].

In our system, two layers comprise a thin stiff skin made of a silicon oxide and a thick foundation made of PDMS. The wavelength and depth of wrinkles increased with increasing plasma conditions such as processing time or bias voltage. This phenomenon may be caused by increasing the thickness and/or the Young's modulus of the silica-like layer [27]. The wrinkles were generally disordered when generated on planar surfaces, but they oriented when formed on prepatterned surfaces. The stress perpendicular to the prepatterns was relieved by expansion, which caused the ripples to orient in the direction perpendicular to our prepatterns (see Fig. 4.5). These oriented wrinkles were related to the disruption of equibiaxial strains (present in flat PDMS surfaces) during plasma treatment [26].

4.4 Discussion

The spontaneously wrinkled patterns on plasma-treated PDMS surfaces can be suppressed through the help of surface prepatterning step. A ripple pattern was not

produced on the prepatterned surfaces even when was exposed to oxygen plasma under a bias voltage of 5 kV for 30 minutes. Ripple patterns were produced in the prepatterned samples when they are subject to an oxygen plasma of bias voltage 10 kV, the orientation of which was perpendicular to the prepattern features. Comparing this result with the control flat PDMS samples treated under identical plasma conditions, the depth of the wrinkling patterns on the prepatterned surfaces was reduced by more than 3 times. Such a prepatterning step, combined with the plasma treatment process, is attractive for potential applications in the system of micro/nano fabrication, which offers a new way to induce ordered compound patterns without using conventional lithographic techniques.

4.5 Summary

In summary, a simple prepatterning step/ plasma treatment to orient spontaneous patterns on PDMS samples was presented. The generated (sub) micron scale features on PDMS samples may be used to order the ripple formation process in the sample. This method for fabricating the oriented wavy structures may be applied in various aspects which include biology, microelectromechanical systems (MEMs) [27] and micro/nano-fabrication[130][131].

Chapter 5. CELL CULTURE ON SURFACE MODIFIED SAMPLES

In this Chapter, cell growth on pristine and plasma-treated PDMS samples was investigated. Prepatterning and plasma ion implantation techniques were both employed for obtaining patterned structures on PDMS samples. For cell investigation experiments, I present osteoblast cells cultured on different prepatterns for cell proliferation investigation. In addition, EAy926 cells were cultured on untreated and plasma treated prepatterns for cell attachment performance studies. Finally, I present the results of HeLa cells alignment and cell spreading on the plasma-treated wrinkle patterns with different sizes.

5.1 Introduction

An understanding of cell behavior on substrates with features is useful for studying natural physiological responses of cells *in vivo*, in order to understand the mechanism of interaction between cells and the extracellular matrix [132][133][134]. There are evidences that microscale and nanoscale patterns have significant effects on cellular behaviour such as cell attachment [135][136], cell proliferation [137] or even cell differentiation [137][138]. Nanogrooved surfaces have been widely studied, and

been found to have great potential in medical devices and tissue engineering [139][140].

PDMS is commonly used for the fabrication of nanogrooved structures for *in vitro* studies, due to its biocompatibility and convenience for prototyping [33]. Moreover, it has been reported that cell adhesion of certain cell lines on PDMS surfaces could be improved by O_2-plasma treatment [141]. Although many studies have been carried out to investigate the relations between cell behavior and features of patterned surfaces, there are few works focusing on the effect of prepatterned surfaces combined with oxygen plasma treatment. Thus, it is important to study the effect of oxygen plasma ion implantation on nanogrooved PDMS samples in investigating the cellular behavior.

5.2 Osteoblasts cells cultured on different prepatterns

5.2.1 Sample preparation and cell culture for proliferation test

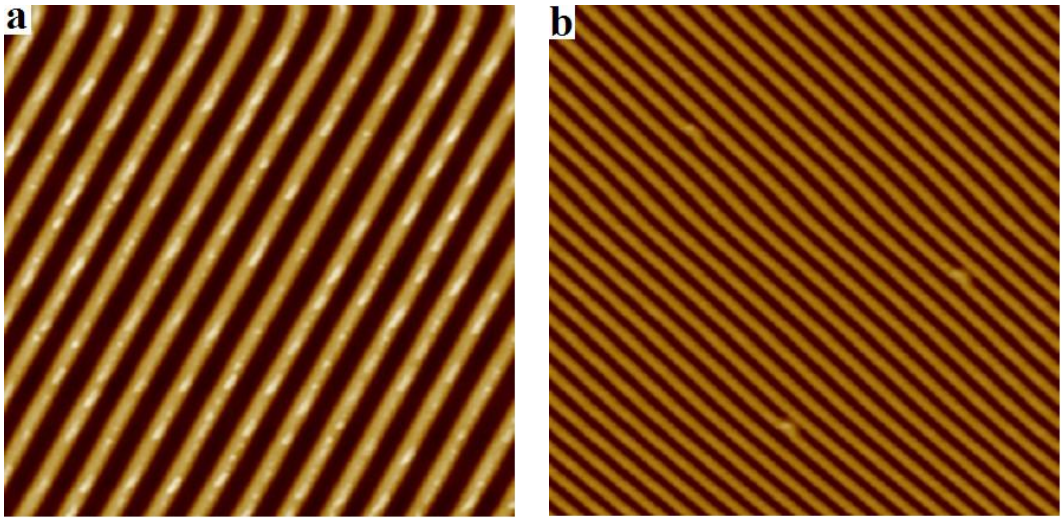

Fig. 5.1 AFM images of PDMS sample surfaces with nanogrooves of different sizes. (a) Tracks of period (height) 1.5 μm (140 nm); and (b) tracks of period (height) 0.75 μm (105 nm). Scan areas and z range of the images are (20 μm × 20 μm 300 nm, respectively.

Different prepatterns with tracks of period (heights) 1.5 μm (140 nm) and 0.75 μm (105 nm) were transferred on the PDMS sample surfaces through a simple prepatterning step as previously described. Fig. 5.1 shows the AFM images of nanogrooves of different sizes generated on PDMS surfaces.

Before cell culture, all the samples were sterilized in 75% ethanol overnight and then cleaned with PBS three times. For observing the proliferation of the MC3T3-E1 osteoblasts cells on the control flat PDMS surface and prepatterned surfaces, approximately 4×10^4 cells were cultured in each well and the culturing medium was refreshed every 3 days. After finishing culturing cells for 1,3, and 6 days, all the samples with the seeded cells were rinsed with sterile PBS solution and then transferred to a new 24-well tissue culture plate.

5.2.2 Osteoblasts cells proliferation results and discussion

A cell count kit (CCK-8 Beyotime, China) was used to investigate the viable cells quantitatively. CCK-8 kit is commonly used to detect cell proliferation by utilizing Dojindo's highly water-soluble tetrazolium salt. WST-8 [2-(2-methoxy-4-nitrophenyl)-3-(4-nitrophenyl)-5-(2,4-disulfophenyl)-2H-tetrazolium, monosodium salt] was reduced by dehydrogenases in the cells at the presence of an electron mediator, releasing an orange-colored formazan in cell culture medium. The amount of the formazan dye produced by dehydrogenases in cells is proportional to the number of viable cells.

The culture medium with 10% CCK was added to those samples in a separate volume of 0.4 mL. After incubation for 4 hours in the dark, the solution was aspirated

and 0.1 mL of solution in each sample was absorbed into the 96-well culture plates. The absorbance can be measured on a power wave micro-plate spectrophotometer (BioTek, USA) with a wavelength of 450 nm. Three samples were prepared for each type group (control flat surface, 750 nm and 1.5 μm tracks), and each sample had three parallel replicas at each time point for CCK test.

5.2.3 Results and discussion

Fig. 5.2 shows the cell proliferation of mouse MC3T3-E1 osteoblasts after culturing for 1, 3 and 6 days. For MC3T3-E1 osteoblasts cultured on different sample surfaces for 1 day, there was no significant difference between them. But for cells cultured on different samples for 3 days, cell proliferation on prepatterned surfaces were much more pronounced than the control samples. Osteoblast proliferation showed an increasing trend on all different types of samples after 3 days and 6 days of culturing when compared with the situation after 1 day of culturing. The cell number on prepatterned surfaces with tracks of 0.75 μm was much larger than on surfaces with tracks of 1.5 μm after culturing for 3 days. After culturing for 6 days, the cell number continued to increase with the culturing time on different types of samples. The cell number on patterned surfaces with tracks of 1.5 μm was the highest after 6 days. From

the results mentioned above, the highest cell density was observed on prepatterned surfaces with widths of 1.5 μm. It could be concluded that the cell proliferation on PDMS samples up to 3 or 6 days was influenced by surface grooves. Moreover, cell proliferation could be effected by surface grooves with different widths or depths.. This observation is agreeable with the results of Ricci *et al.* [142] and Green et al. [143]. For instance, Green's group reported that abdomen fibroblasts cells cultured on surfaces with 2 μm and 5 μm pillars showed an increasing trend of proliferation. Ricci *et al.* investigated the cell growth of rat tendon fibroblasts and rat bone marrow colonies on surfaces with grooves. The results showed that colony growth rate varied and suggested that surface microgeometries can be utilized to control the growth rate of cells at seeding surfaces. It is possible that the composition and amount of secreted protein deposition was different between cells cultured on flat surfaces and prepatterned surfaces due to discrepancies in local surface energy [94]. This theory was supported by other researches, for example, DIA data which revealed an obvious effect of grooved surface on the growth orientation, size and shape of rat dermal fibroblasts (RDFs) [92].

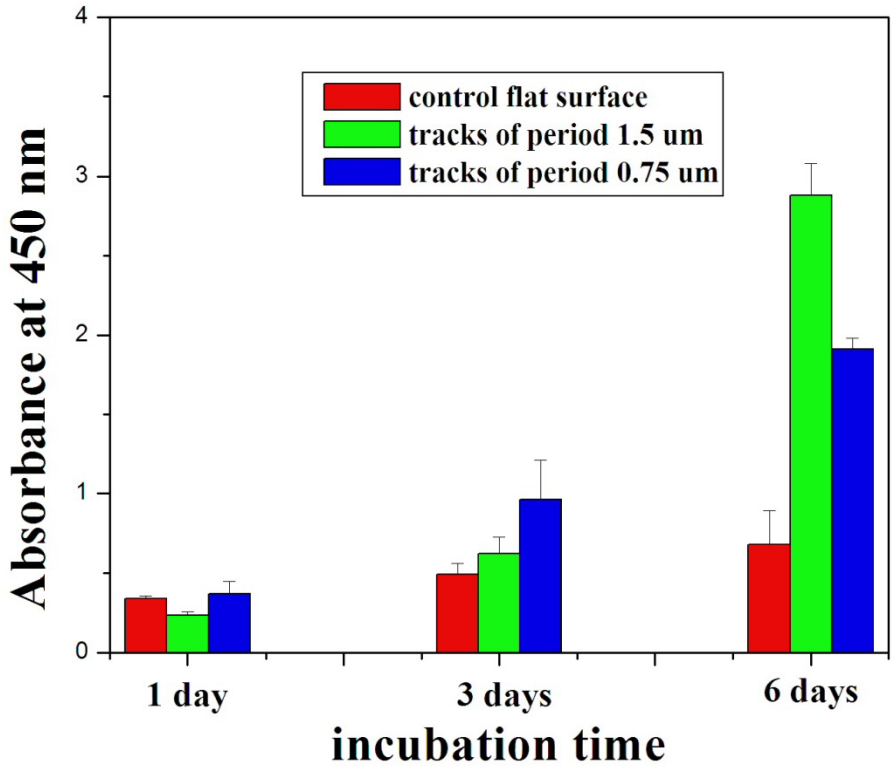

Fig. 5.2 Cell proliferation assay of MC3T3-E1 osteoblasts cells cultured on the control and prepatterned samples for 1, 3 and 6 days.

5.3 EAhy926 cell culture on untreated and plasma-treated prepatterns

5.3.1 Sample preparation and pattern characterization

There are two groups of samples I studied for cell adhesion investigation. The 'untreated group' includes samples of control flat surface, different prepatterns with tracks of period (heights) 1.5 μm (140 nm) and 0.75 μm (105 nm). Pattern characterization images are shown in Fig. 5.1 The 'plasma-treated group' includes

samples with identical starting surface morphologies but were treated by oxygen plasma with a bias voltage of 3 kV for 15 min. Fig. 5.3 shows AFM images of different surface morphologies after treated by plasma ion implantation. After the oxygen plasma treatment process, disordered ripple patterns were found on the control samples (Fig. 5.3 (a)), and no compound structure happened on the prepatterned surfaces. The depth of prepatterned surfaces decreased for different extents. For prepatterned surface with tracks of 1.5 μm (Fig. 5.3(b)), the track depths reduced slightly to to 130 nm (compared with initial depth of 140 nm); while the depth of prepatterned surface with tracks of 0.75 μm changed from 104 nm to 60 nm.

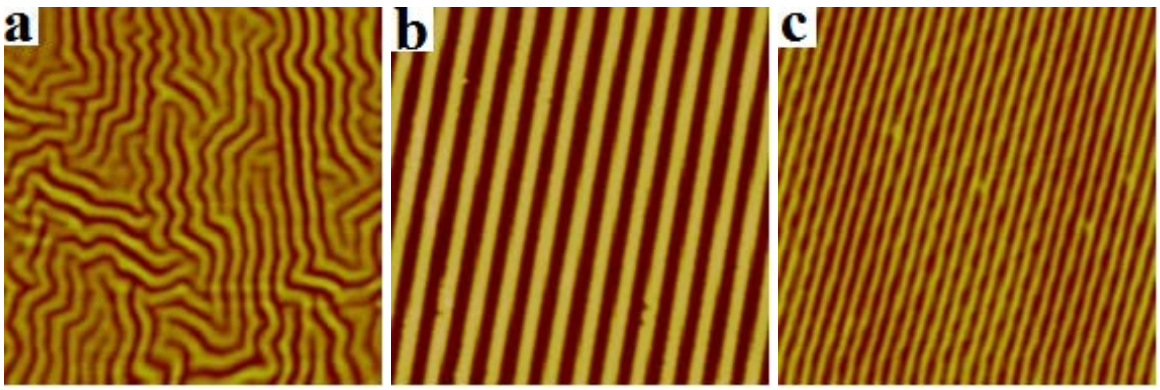

Fig. 5.3 AFM images of 'plasma-treated group' PDMS samples with different initial morphologies, after exposed to 3 kV oxygen plasma for 15 min: control flat surface (a), tracks of periods 1.5 μm (b) and 0.75 μm (c), respectively. For all the images, the scan area is (20 μm×20 μm) and z scale is 200 nm.

5.3.2 Cell adhesion investigation

To investigate cell attachment, untreated and plasma-treated samples were immersed in 2 mL of the cell suspension solution at a density of approximately 20,000 cells/mL for 1, 3, and 6 hours. At each time point, the samples were rinsed with PBS solution carefully to remove loose cells on it, and fixed in 4% paraformaldehyde for 30 min. They were then stained with 40, 60-diamidino-2-phenylindole (DAPI) in the dark for 10 min and then rinsed three times using PBS solution before calculating the cell number from six random fields of each sample surface, using a fluorescence microscope (Zeiss).

5.3.3 Results and discussions

Fig. 5.4 illustrates the endothelium cell adhesion on regular patterned PDMS surfaces as compared with plasma treated patterned PDMS surfaces. As shown in the image, the number of adhering endothelium cell increases with time, and there are more cells on the regular patterned PDMS surface. That implies endothelium cells adhered well to the regular patterned PDMS surface. In contrast, plasma-treated groups significantly inhibited cell adhesion. However, it should be noted that at the 6-hr point the number of endothelium cells adhering on the prepattern with tracks of 750 nm did not show statistically significant differences as compared with untreated samples. The

decreased number of cells adhering to the sample could be due to the oxygen plasma process, which generated a lot of oxygen free radicals. Such unstable end-groups are destructive for membrane proteins, and therefore cell connection to substrate material was disturbed [144][145][146][147].

In the literatures, PDMS regular patterns are suggested suitable for endothelial cell growth without any reagents, and can form a dense monolayer of cells [148][149]. My test proved that the current oxygen plasma treatment technology needs to be optimized, as this technology does not significantly promote endothelial cell adhesion. For most cell kinds such as endothelium cells, cell attachment to substrates is important to their survival. In the attachment process, the cells recognize the particular ligands on the adsorbed proteins (like RGD amino acid sequence) by the integrin receptors which are on the cell membranes part. The integrin is made up of both transmembranes α and β subunits, which can transfer cell information to intra- and extra-cellular environments to regulate cell attachment, morphology and viability [150][151]. There are three main adhesive interactions between cells and implant surfaces, namely focal adhesion, close contact, and extracellular matrix contact. In these three types of interactions, the focal adhesion has the shortest distance (10–20 nm) between the cells and implant surfaces, so it has the strongest adhesive force [152][153]. The surface energy, chemistry

composition, and morphology may affect the structure, formation, area, and composition of focal adhesion via varying integrins expressions and binding [154][155][156]. Hydrophilic and neutral implant surfaces can accelerate the formation of focal adhesion and the subsequent cell adhesion [157].

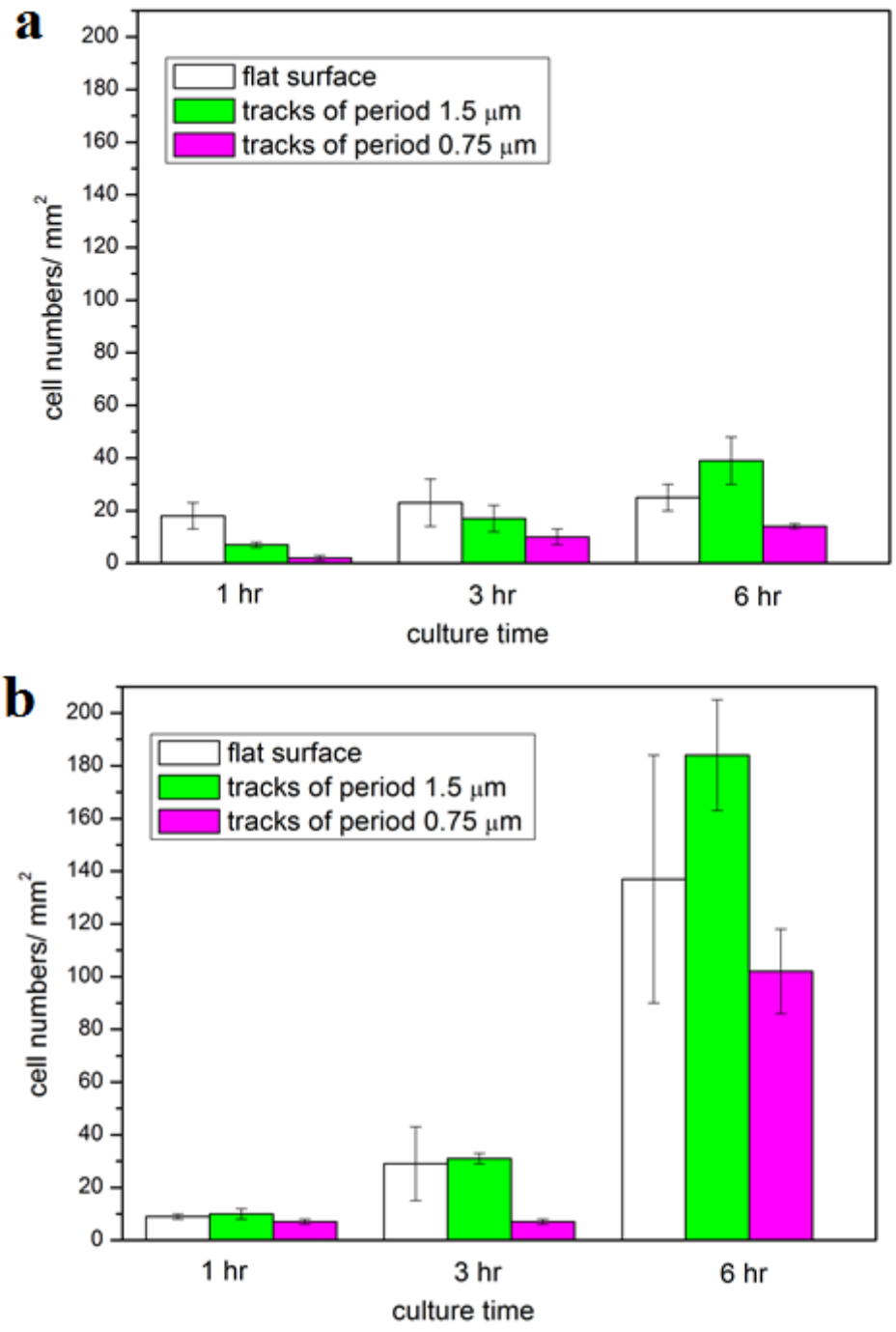

Fig. 5.4 Adhesion of endothelial cells on untreated sample group (a) and plasma-treated sample group (b). Each group has three type of samples: flat surface, tracks of period 1.5 μm and tracks of period 0.75 μm.

5.4 HeLa cells cultured on treated patterns

5.4.1 Cell elongation and cell alignment

For quantitative analysis of cell alignment, aspect ratio and cell spreading on different samples, I extracted the behaviour of individual cells on different sample surfaces from stained actin fibers of cells.

The software ImageJ was used for analyzing cell information [158]. First, cell cytoskeleton was highlighted and outlined by adjusting threshold values of images (such as brightness) in ImageJ. From the outlined shapes, cell information such as cell angle, major axis length, minor axis length (best-fitted into an eclipse) and cell spreading area were automatically determined by the computer. In the statistical process, the angles were adjusted from 0-180 to 0-90 degrees. The collective angles were averaged to get a mean angle. If the cell angle was equal to zero, the cell showed perfect alignment with external features; if the angle was less than 15 degree, I considered the cell aligned parallel to the groove; if the angle was larger 85 degree, I considered the cell aligned perpendicular to the grooves. Cell elongation was evaluated as the ratio of major axis length and minor axis length. Cell alignment was defined by the angle between the long axis of cell and the reference direction. In this experiment,

groove direction was regarded as the reference direction.

Fig. 5.5 (a) to (c) shows the overview of measurement of cell morphology characteristics. For the alignment angle, the orientation was examined by determining the angle α between the major axis and groove direction or the reference direction (Fig.5.5(a)). The aspect ratio was calculated as the major axis length divided by the minor axis length (the maximal length perpendicular to the major axis) (Fig.5.5 (b)). Cell spreading area, which is shown in Fig. 5.3(c), is measured through drawing the boundary line of cells and measuring the total surface area by ImageJ software.

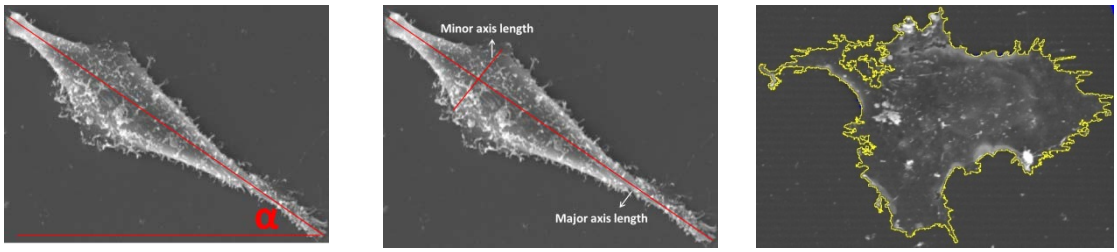

(a) **(b)** **(c)**

Fig. 5.5 Overview of different types of cell morphologies characteristic measurements. (a) Alignment angle α, (b) cell aspect ratio (major axis length/ minor axis length), and (c) cell spreading area.

5.4.2 HeLa cells cultured on untreated and plasma-treated surfaces

Fig. 5.6 is the SEM images of cell cultured on prepatterned surfaces and plasma-treated (bias voltage5 kV for 15 min) prepatterned surface for 24 hours. From Fig. 5.6,

it can be seen that prepatterned PDMS substrates induce significant cell alignment and lead to cells with high aspect ratios. There is no significant increase in the cell spreading area as compared with plasma-modified prepatterns. Cells cultured on plasma-modified prepatterned surfaces (Fig. 5.6 (b)) reveals a slight but unobvious alignment with low aspect ratio, and the highest spreading area among all samples. Fig. 5.7 shows SEM images of cells cultured on control flat surface and plasma treated surfaces with different bias voltages (5 kV/10 kV) for 15 min. Plasma-treated surfaces did not result in preferential cell alignment. The result of cell alignment in the plasma-treated substrates group shows that 5 kV plasma-treated substrate group (Fig. 5.7 (b)) does not result in alignment, with an increased spreading area of the cells. Substrates treated with a bias voltage of 10 kV (Fig. 5.7 (c)) also do not show cell alignment, and the cell spreading is not significantly different from that of the flat surfaces and prepatterned surfaces. The amount of cells on sample surfaces was observed to be small. Cell growth was retarded on this kind of sample surface.

The plasma-treated surfaces have a significant effect on the spreading area of the cells. Substrates undergone plasma ion implantation have significantly enhanced the spreading area compared with the groups without any plasma ion implantation. However, flat surfaces treated by plasma with bias voltage of 10 kV for 15 min did not

encourage cell spreading. Besides, the amount of cells on this kind of substrate was the smallest among groups. It is inferred that the ripple patterns on sample surfaces is apoptosis inducing. In addition, the aspect ratio of cells was smaller on plasma-treated substrates. For plasma-modified prepattern and control surfaces using a bias voltage of 5 kV, it may be resulted from the effect of improved cell spreading. For control surface plasma-treated with a bias voltage of 10 kV, it could be that the random-oriented wrinkle patterns reduce the cell motility / persistence of movement. In prepatterned substrates, the directional growth can be explained by contact guidance phenomenon [159] that cell cultured on micro/nanogrooved patterns, these parallel grooves will adjust cell growth direction and guide cell alignment along patterns.

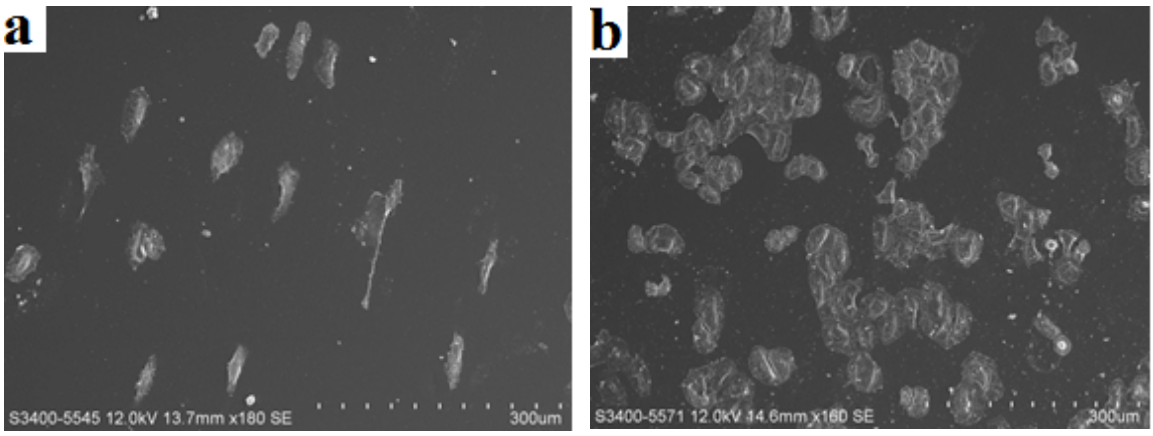

Fig. 5.6 SEM images of HeLa cells cultured for 24 hours on untreated prepatterned substrates (a), and on 15 min 5-kV plasma modified prepatterned substrates (b).

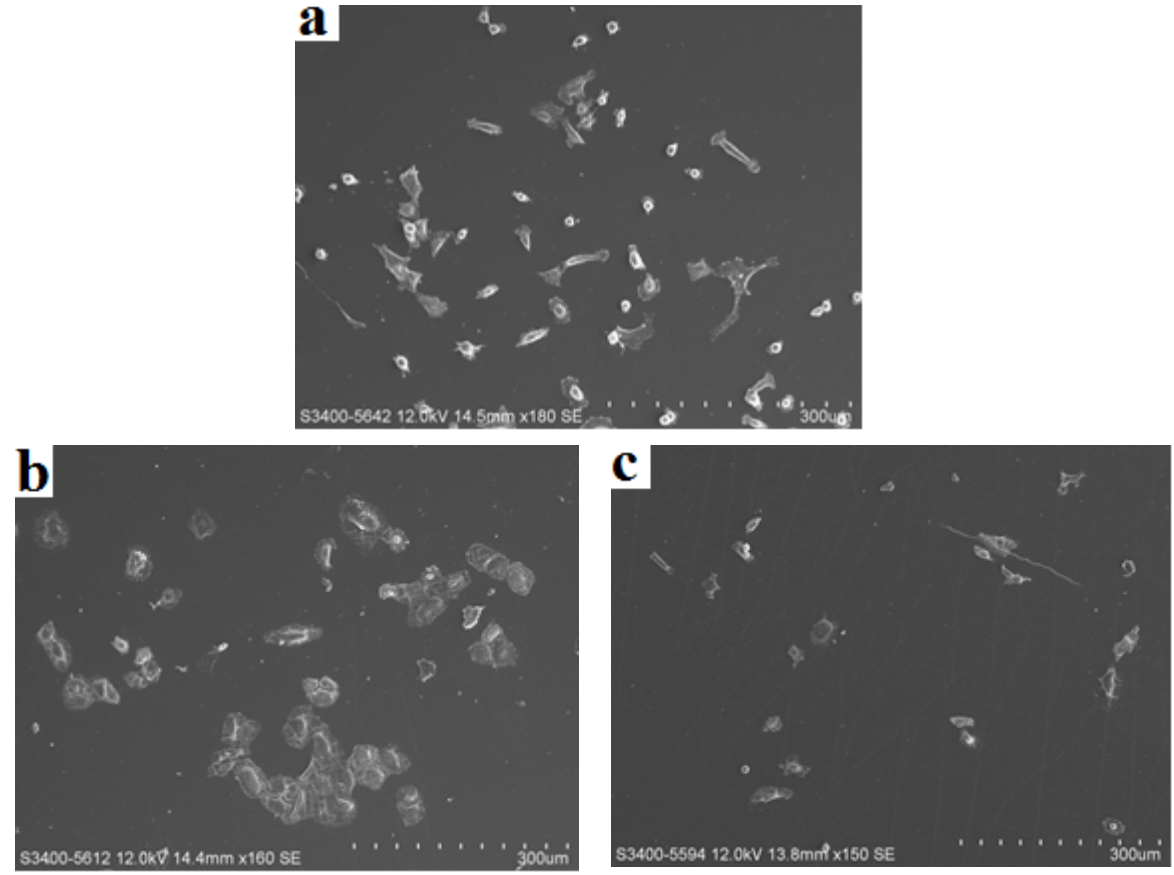

Fig. 5.7 SEM images of HeLa cells cultured for 24hours on flat substrates (a), plasma modified flat surfaces with bias voltage of 5 kV for 15 min (b), and plasma modified flat surfaces with bias voltage of 10 kV for 15 min (c).

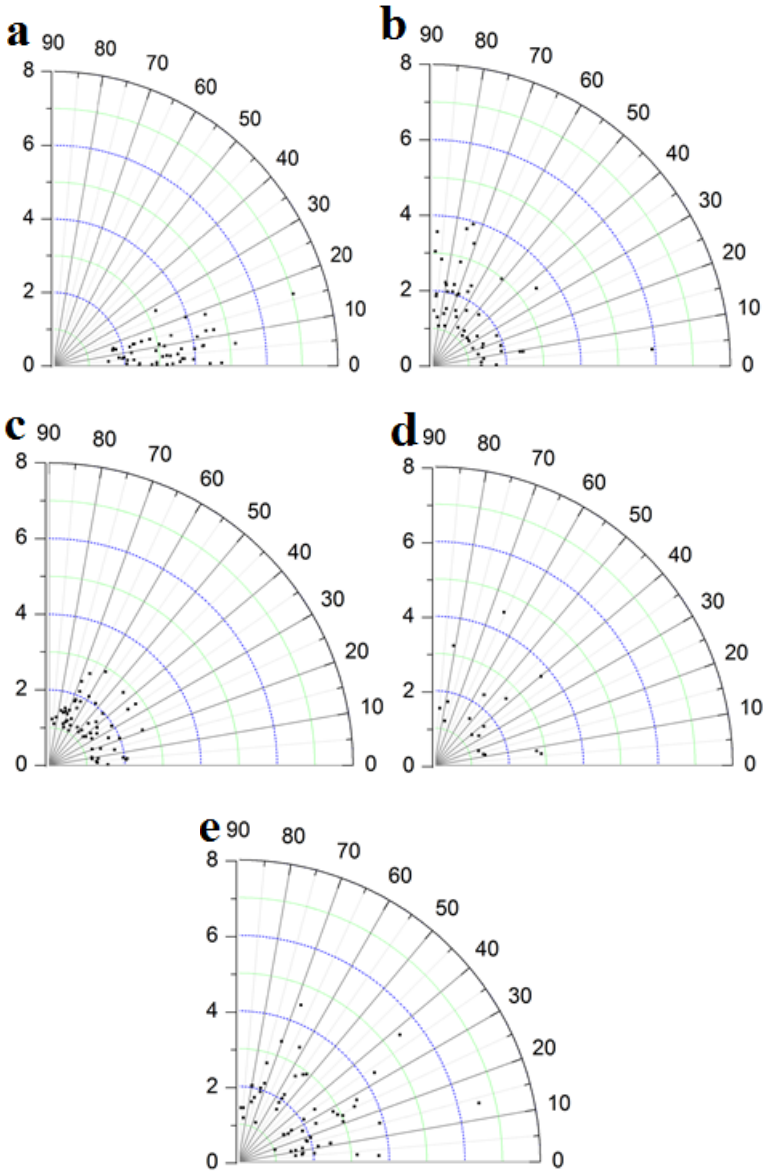

Fig. 5.8 Polar plots of cell alignment (angular coordinate) and elongation (radial coordinate) of HeLa cells cultured on different sample surfaces. Cells cultured on nanogrooved surface without O_2-plasma treatment (a), nanogrooved surface treated with low-voltage O_2 plasma (b), flat surface treated with low-voltage O_2-plasma (c), flat surface treated with high-voltage O_2-plasma (d) and flat control surface (e) for 24 hrs.

5.4.3 Discussion of HeLa cell growth comparison on different surfaces

In this research, I studied the cellular behavior of mammalian cell line HeLa on five different kinds of substrate surfaces, including flat control surface (without O_2-plasma treatment), low-voltage O_2-plasma treated flat surface (5 kV, 15 min), high-voltage O_2-plasma treated flat surface (10 kV, 15 min), nanogrooved surface structure (1.5 μm in groove width and spacing width) without O_2-plasma treatment, and nanogrooved surface structure (1.5 μm in groove width and spacing width) with O_2-plasma treatment (5 kV, 15 min). Cell spreading area, cell elongation, and cell alignment angle were measured and analyzed.

As illustrated in Fig. 5.9 (a) and (b), my results indicated that the nanogrooved surfaces without O_2-plasma treatment were very effective in promoting cell alignment and elongation. On the other hand, in Fig. 5.9 (c) cells on the flat surface treated with low-voltage O_2-plasma showed significantly larger cell spreading area than the cells on the flat surface either with high-voltage plasma treatment or without any treatment. Although the cells on the O_2-plasma treated nanogrooved surfaces display larger spreading area than on the nanogrooved surface without O_2-plasma treatment, the cell elongation and alignment were similar to those on the flat control surfaces. In addition, high-magnification scanning electron microscopy (SEM) images showed that high-

voltage O_2-plasma treatment generated random microstructures on the flat PDMS surface (Fig. 5.7), which may be the reason for the decrease of cell spreading area on the high-voltage O_2-plasma treated surface.

Overall, a nanogrooved surface promotes cell elongation and alignment while low-voltage O_2-plasma treatment promotes cell spreading. However, O_2-plasma treatment disrupts the ability of nanogrooved surfaces to enhance cell elongation and alignment. Hence, O_2-plasma treatment can interrupt the contact guidance effect of nanogrooved PDMS surfaces, which must be considered during fabrication of medical devices.

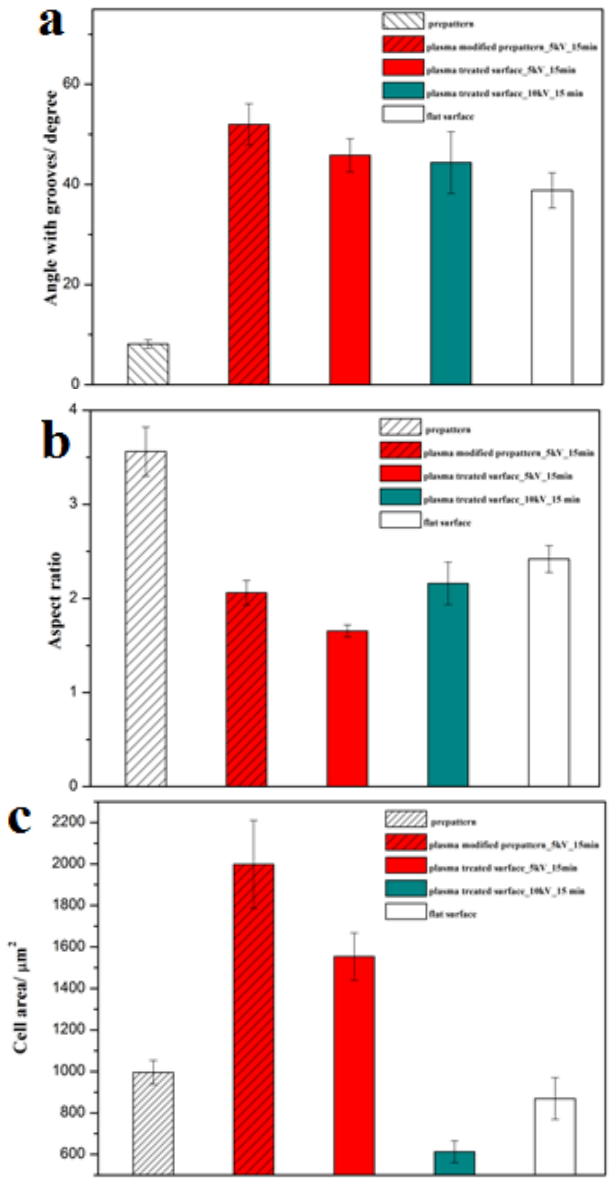

Fig. 5.9 Cell alignment (a), cell elongation (b) and spreading area (c) of cells cultured on flat control surface (white column), flat surface treated with low-voltage O_2-plasma (red column), flat surface treated with high-voltage O_2-plasma (green column), nanogrooved surface without O_2-plasma treatment (white strip column), and nanogrooved surface treated with low-voltage O_2 plasma (red strip column) for 24 hrs.

5.5 Summary

In this Chapter, high-resolution nanopatterns were fabricated and underwent plasma treatment. HeLa cells, bone cells and Eahy926 cells were cultured on the patterns. We found that for the given geometry HeLa cells were aligned in the nanogrooves directions, showing the effect of geometric confinement on the resulting cell elongation and alignment. It indicated that the prepatterning step, combined with plasma treatment, are relevant for more clear understanding of cell adhesion and migration behaviors on patterned surfaces.

Chapter 6 Conclusions and Future Work

6.1 Summary of major results

The research work in this M.Phil. project included the study of wrinkling behavior on PDMS surfaces by plasma treatment, of which ordered patterns can be achieved through a prepatterning step combined with appropriate plasma ion implantation conditions. Potential biological applications of such featured substrates have been demonstrated.

The effects of plasma treatment parameters, like processing time and bias voltage, as well as prepattern geometries, on the surface morphology changes of PDMS subjected to plasma ion implantation were characterized by AFM. By means of the surface prepatterning step, spontaneous ripple waves generated by plasma treatment can be suppressed. For example, disordered waves were not induced on prepatterned surfaces (tracks of 1.5 μm and 140 nm) even when it was treated by plasma ion implantation with the bias voltage of 5 kV for 30 min , while ripples can be observed on control surfaces (without prepatterning) when they were just deposited at the oxygen plasma atmosphere without applied bias voltage. The development of hierarchal wavy patterns could also be controlled through the combined prepatterning/ plasma treatment.

When ripple waves appeared in the prepatterned substrates after implantation with high bias voltages (10 kV), the induced spontaneous ripples were oriented at the direction which is perpendicular to the prepatterns. Comparing it with control flat surfaces which were treated by plasma ion implantation at the same processing conditions, the depth of the induced waves developing on prepatterned surfaces was decreased by more than 3 times.

For the biological cell-growth investigations, grooved pattern was detected by cells and led to the “contact guidance” phenomena, where HeLa cells could align themselves according to the surface grooves. In Chapter 5, my results indicated that the nanogrooved surfaces without plasma treatment were very effective in promoting cell alignment and elongation. But after oxygen plasma treatment, the cell elongation and alignment on prepatterned surfaces were similar to those on the control flat surface. Moreover, high-magnification scanning electron microscopy (SEM) images have showed that random microstructures of PDMS (induced by plasma ion implantation under high bias voltages) decreased cell spreading area. Also, the amount of cells on this kind of substrate was the smallest among groups. It suggested that the spontaneous ripple patterns induced by the plasma treatment was apoptosis inducing. The difference in groove widths and depths influenced osteoblast cells proliferation and endothelium

adhesion. The highest osteoblasts cell density was observed on prepatterned surfaces with tracks width of 1.5 μm after culturing for 6 days. Osteoblasts cell proliferation on PDMS samples was influenced by surface grooves, as compared with cell behavior on control flat surfaces.

6.2 Future work

In this work, the surface morphology changes of PDMS were studied. Some further investigations are needed. For instance, the prepattern with tracks of period (depth) 1.5 μm (140nm) showed an increased variation when implanted at bias voltage of 5 kV. This special behavior, combined with the absence of spontaneously ripple patterns on the sample surface, require more in-depth analysis. Further experiments with more bias voltage parameters can be done for obtaining detailed prepattern variation trend. Such a systematic study is important, because wrinkling is a significant mechanical phenomenon which can induce periodic surfaces, ranging from randomly-oriented to well-oriented waves, as a consequence of the relaxation of isotropic and anisotropic stresses, respectively.

In addition, the surface wettability change of PDMS after oxygen plasma treatment needs more experimental support, which could be observed by calculating the contact

angle. The hydrophobic property of PDMS and fast hydrophobic recovery of PDMS even after surface hydrophilization-treatment negatively influences the performance and properties of PDMS-based microfluidic devices. Hence, surface modification of PDMS samples, especially on improving hydrophilic stability, will be beneficial for microfluidic applications.

Moreover, more experiments on the influence of prepattern parameters on cell growth are needed for exploring influencing factors (width or depth) on cell behavior. From my preliminary results, it may be concluded that the cell behavior was influenced by the surface grooves. Further investigations on the cell numbers or morphology on surfaces with different groove widths could be made, which can be helpful for understanding cell growth on prepatterned surfaces.

References

1. Fu, R. K. Y.; Cheung, I. T. L.; Mei, Y. F.; Shek, C. H.; Siu, G. G.; Chu, P. K.; Yang, W. M.; Leng, Y. X.; Huang, Y. X.; Tian, X. B.; Yang, S. Q., Surface modification of polymeric materials by plasma immersion ion implantation. *Nucl Instrum Meth B* **2005,** *237* (1-2), 417-421.

2. Wu, D. Y.; Meure, S.; Solomon, D., Self-healing polymeric materials: A review of recent developments. *Prog Polym Sci* **2008,** *33* (5), 479-522.

3. Sabir, M. I.; Xu, X. X.; Li, L., A review on biodegradable polymeric materials for bone tissue engineering applications. *J Mater Sci* **2009,** *44* (21), 5713-5724.

4. Deng, T.; Wu, H. K.; Brittain, S. T.; Whitesides, G. M., Prototyping of masks, masters, and stamps/molds for soft lithography using an office printer and photographic reduction. *Anal Chem* **2000,** *72* (14), 3176-3180.

5. Quake, S. R.; Scherer, A., From micro- to nanofabrication with soft materials. *Science* **2000,** *290* (5496), 1536-1540.

6. Beck, W. H., Pyrolysis Studies of Polymeric Materials Used as Binders in Composite Propellants - a Review. *Combust Flame* **1987,** *70* (2), 171-190.

7. Guo, L. J., Nanoimprint lithography: Methods and material requirements. *Adv Mater* **2007,** *19* (4), 495-513.

8. Despa, M. S.; Kelly, K. W.; Collier, J. R., Injection molding of polymeric LIGA HARMs. *Microsyst Technol* **1999,** *6* (2), 60-66.

9. Duffy, D. C.; McDonald, J. C.; Schueller, O. J. A.; Whitesides, G. M., Rapid prototyping of microfluidic systems in poly(dimethylsiloxane). *Anal Chem* **1998,** *70* (23), 4974-4984.

10. Wu, C. H.; Chen, C. H.; Fan, K. W.; Hsu, W. S.; Lin, Y. C., Design and fabrication of polymer microfluidic substrates using the optical disc process. *Sensor Actuat a-Phys* **2007,** *139* (1-2), 310-317.

11. Lin, L.; Cheng, Y. T.; Chiu, C. J., Comparative study of hot embossed micro structures fabricated by laboratory and commercial environments. *Microsyst Technol* **1998,** *4* (3), 113-116.

12. Wei, G. H.; Bhushan, B.; Ferrell, N.; Hansford, D., Microfabrication and nanomechanical characterization of polymer microelectromechanical system for biological applications. *J Vac Sci Technol A* **2005,** *23* (4), 811-819.

13. Toth, A.; Kereszturi, K.; Mohai, M.; Bertoti, I., Plasma based ion implantation of engineering polymers. *Surf Coat Tech* **2010,** *204* (18-19), 2898-2908.

14. Paguirigan, A. L.; Beebe, D. J., From the cellular perspective: exploring differences in the cellular baseline in macroscale and microfluidic cultures. *Integr Biol* **2009,** *1* (2), 182-195.

15. Mutel, B.; Grimblot, J.; Dessaux, O.; Goudmand, P., XPS investigations of nitrogen-plasma-treated polypropylene in a reactor coupled to the spectrometer. *Surf Interface Anal* **2000,** *30* (1), 401-406.

16. Grace, J. M.; Gerenser, L. J., Plasma treatment of polymers. *J Disper Sci Technol* **2003,** *24* (3-4), 305-341.

17. Fu, R. K. Y.; Mei, Y. F.; Wan, G. J.; Siu, G. G.; Chu, P. K.; Huang, Y. X.; Tian, X. B.; Yang, S. Q.; Chen, J. Y., Surface composition and surface energy of Teflon treated by metal plasma immersion ion implantation. *Surf Sci* **2004,** *573* (3), 426-432.

18. Antipov, A. A.; Sukhorukov, G. B., Polyelectrolyte multilayer capsules as vehicles with tunable permeability. *Adv Colloid Interfac* **2004,** *111* (1-2), 49-61.

19. Zhou, J. W.; Ellis, A. V.; Voelcker, N. H., Recent developments in PDMS surface modification for microfluidic devices. *Electrophoresis* **2010,** *31* (1), 2-16.

20. Roman, G. T.; Hlaus, T.; Bass, K. J.; Seelhammer, T. G.; Culbertson, C. T., Sol-gel modified poly(dimethylsiloxane) microfluidic devices with high electroosmotic Mobilities and hydrophilic channel wall characteristics. *Anal Chem* **2005,** *77* (5), 1414-1422.

21. Chu, P. K., Enhancement of surface properties of biomaterials using plasma-based technologies. *Surf Coat Tech* **2007,** *201* (19-20), 8076-8082.

22. Chu, P. K.; Chen, J. Y.; Wang, L. P.; Huang, N., Plasma-surface modification of biomaterials. *Mat Sci Eng R* **2002,** *36* (5-6), 143-206.

23. Conrad, J. R.; Radtke, J. L.; Dodd, R. A.; Worzala, F. J.; Tran, N. C., Plasma Source Ion-Implantation Technique for Surface Modification of Materials. *J Appl Phys* **1987,** *62* (11), 4591-4596.

24. Wang, H. Y.; Kwok, D. T. K.; Wang, W.; Wu, Z. W.; Tong, L. P.; Zhang, Y. M.; Chu, P. K., Osteoblast behavior on polytetrafluoroethylene modified by long pulse, high frequency oxygen plasma immersion ion implantation. *Biomaterials* **2010,** *31* (3), 413-419.

25. Ostrikov, K.; Cvelbar, U.; Murphy, A. B., Plasma nanoscience: setting directions, tackling grand challenges. *J Phys D Appl Phys* **2011,** *44* (17).

26. Chua, D. B. H.; Ng, H. T.; Li, S. F. Y., Spontaneous formation of complex and ordered structures on oxygen-plasma-treated elastomeric polydimethylsiloxane. *Appl Phys Lett* **2000,** *76* (6), 721-723.

27. Bowden, N.; Huck, W. T. S.; Paul, K. E.; Whitesides, G. M., The controlled formation of ordered, sinusoidal structures by plasma oxidation of an elastomeric polymer. *Appl Phys Lett* **1999,** *75* (17), 2557-2559.

28. Schmalenberg, K. E.; Buettner, H. M.; Uhrich, K. E., Microcontact printing of proteins on oxygen plasma-activated poly(methyl methacrylate). *Biomaterials* **2004,** *25* (10), 1851-1857.

29. L.E., M. E. S., Cell responses to plasma polymers-implications for wound care. *Wound Practice and Research* **2012,** *20* (2), 74-79.

30. Smetana, K.; Vacik, J.; Dvorankova, B., Interaction of cells with polymers. *Macromol Symp* **1996,** *109*, 145-153.

31. Kaufmann, T.; Ravoo, B. J., Stamps, inks and substrates: polymers in microcontact printing. *Polym Chem-Uk* **2010,** *1* (4), 371-387.

32. Mata, A.; Fleischman, A. J.; Roy, S., Characterization of polydimethylsiloxane (PDMS) properties for biomedical micro/nanosystems. *Biomed Microdevices* **2005,** *7* (4), 281-293.

33. Belanger, M. C.; Marois, Y., Hemocompatibility, biocompatibility, inflammatory and in vivo studies of primary reference materials low-density polyethylene and polydimethylsiloxane: A review. *J Biomed Mater Res* **2001,** *58* (5), 467-477.

34. Jaeger, R. D.; Gleria, M., *Inorganic polymers*. Nova Science Publishers: New York, 2007; p viii, 925 p.

35. Hua, F.; Sun, Y. G.; Gaur, A.; Meitl, M. A.; Bilhaut, L.; Rotkina, L.; Wang, J. F.; Geil, P.; Shim, M.; Rogers, J. A.; Shim, A., Polymer imprint lithography with molecular-scale resolution. *Nano Lett* **2004,** *4* (12), 2467-2471.

36. Sollier, E.; Murray, C.; Maoddi, P.; Di Carlo, D., Rapid prototyping polymers for microfluidic devices and high pressure injections. *Lab Chip* **2011,** *11* (22), 3752-3765.

37. Charati, S. G.; Stern, S. A., Diffusion of gases in silicone polymers: Molecular dynamics simulations. *Macromolecules* **1998,** *31* (16), 5529-5535.

38. Leclerc, E.; Sakai, Y.; Fujii, T., Cell culture in 3-dimensional microfluidic structure of PDMS (polydimethylsiloxane). *Biomed Microdevices* **2003,** *5* (2), 109-114.

39. Piruska, A.; Nikcevic, I.; Lee, S. H.; Ahn, C.; Heineman, W. R.; Limbach, P. A.; Seliskar, C. J., The autofluorescence of plastic materials and chips measured under laser irradiation. *Lab Chip* **2005,** *5* (12), 1348-1354.

40. Bashir, R., BioMEMS: state-of-the-art in detection, opportunities and prospects. *Adv Drug Deliver Rev* **2004,** *56* (11), 1565-1586.

41. Rebello, K. J., Applications of MEMS in surgery. *P Ieee* **2004,** *92* (1), 43-55.

42. Roy, S.; Ferrara, L. A.; Fleischman, A. J.; Benzel, E. C., Microelectromechanical systems and neurosurgery: A new era in a new millennium. *Neurosurgery* **2001,** *49* (4), 779-797.

43. Mata, A.; Su, X. W.; Fleischman, A. J.; Roy, S.; Banks, B. A.; Miller, S. K.; Midura, R. J., Osteoblast attachment to a textured surface in the absence of exogenous adhesion proteins. *Ieee T Nanobiosci* **2003,** *2* (4), 287-294.

44. Mukhopadhyay, R., when PDMS isn't the best. *analytical chemistry* **2007,** *79* (9), 3249-3253.

45. Gotoh, K.; Nakata, Y.; Tagawa, M.; Tagawa, M., Wettability of ultraviolet excimer-exposed PE, PI and PTFE films determined by the contact angle measurements. *Colloid Surface A* **2003,** *224* (1-3), 165-173.

46. Makamba, H.; Kim, J. H.; Lim, K.; Park, N.; Hahn, J. H., Surface modification of poly(dimethylsiloxane) microchannels. *Electrophoresis* **2003,** *24* (21), 3607-3619.

47. Niu, Z. Q.; Gao, F.; Jia, X. Y.; Zhang, W. P.; Chen, W. Y.; Qian, K. Y., Synthesis studies of sputtering TiO2 films on poly(dimethylsiloxane) for surface modification. *Colloid Surface A* **2006,** *272* (3), 170-175.

48. Feng, J. T.; Zhao, Y. P., Influence of different amount of Au on the wetting behavior of PDMS membrane. *Biomed Microdevices* **2008,** *10* (1), 65-72.

49. Zhang, Q.; Xu, J. J.; Liu, Y.; Chen, H. Y., In-situ synthesis of poly(dimethylsiloxane)-gold nanoparticles composite films and its application in microfluidic systems. *Lab Chip* **2008,** *8* (2), 352-357.

50. Makamba, H.; Hsieh, Y. Y.; Sung, W. C.; Chen, S. H., Stable permanently hydrophilic protein-resistant thin-film coatings on poly(dimethylsiloxane) substrates by electrostatic self-assembly and chemical cross-linking. *Anal Chem* **2005,** *77* (13), 3971-3978.

51. Roman, G. T.; Culbertson, C. T., Surface engineering of poly(dimethylsiloxane) microfluidic devices using transition metal sol-gel chemistry. *Langmuir* **2006,** *22* (9), 4445-4451.

52. Slentz, B. E.; Penner, N. A.; Lugowska, E.; Regnier, F., Nanoliter capillary electrochromatography columns based on collocated monolithic support structures molded in poly(dimethyl siloxane). *Electrophoresis* **2001,** *22* (17), 3736-3743.

53. Roman, G. T.; McDaniel, K.; Culbertson, C. T., High efficiency micellar electrokinetic chromatography of hydrophobic analytes on poly(dimethylsiloxane) microchips. *Analyst* **2006,** *131* (2), 194-201.

54. Liu, X. Y.; Chu, P. K.; Ding, C. X., Surface modification of titanium, titanium alloys, and related materials for biomedical applications. *Mat Sci Eng R* **2004,** *47* (3-4), 49-121.

55. Alterkop, B. A.; Rukhadze, A. A., Stationary Nonlinear Ion-Acoustic Oscillations in a Dense Weakly Ionized Current-Carrying Plasma. *Zh Eksp Teor Fiz+* **1972,** *62* (3), 989-&.

56. Liu, Y. J.; Ganser, D.; Schneider, A.; Liu, R.; Grodzinski, P.; Kroutchinina, N., Microfabricated polycarbonate CE devices for DNA analysis. *Anal Chem* **2001,** *73* (17), 4196-4201.

57. Chen, X.; Cui, D. F.; Wang, L.; Wang, M.; Zhao, Q., Development and characterization of DNA hybridization reaction on PDMS microchip. *Int J Nonlinear Sci* **2002,** *3* (3-4), 211-214.

58. Lee, S. J.; Lee, S. Y., Micro total analysis system (mu-TAS) in biotechnology. *Appl Microbiol Biot* **2004,** *64* (3), 289-299.

59. Toriello, N. M.; Liu, C. N.; Mathies, R. A., Multichannel reverse transcription-polymerase chain reaction microdevice for rapid gene expression and biomarker analysis. *Anal Chem* **2006,** *78* (23), 7997-8003.

60. Bodas, D.; Khan-Malek, C., Hydrophilization and hydrophobic recovery of PDMS by oxygen plasma and chemical treatment - An SEM investigation. *Sensor Actuat B-Chem* **2007,** *123* (1), 368-373.

61. Vickers, J. A.; Caulum, M. M.; Henry, C. S., Generation of hydrophilic poly(dimethylsiloxane) for high-performance microchip electrophoresis. *Anal Chem* **2006,** *78* (21), 7446-7452.

62. Hillborg, H.; Ankner, J. F.; Gedde, U. W.; Smith, G. D.; Yasuda, H. K.; Wikstrom, K., Crosslinked polydimethylsiloxane exposed to oxygen plasma studied by neutron reflectometry and other surface specific techniques. *Polymer* **2000,** *41* (18), 6851-6863.

63. Zhou, J. W.; Khodakov, D. A.; Ellis, A. V.; Voelcker, N. H., Surface modification for PDMS-based microfluidic devices. *Electrophoresis* **2012,** *33* (1), 89-104.

64. Ren, X. Q.; Bachman, M.; Sims, C.; Li, G. P.; Allbritton, N., Electroosmotic properties of microfluidic channels composed of poly(dimethylsiloxane). *J Chromatogr B* **2001,** *762* (2), 117-125.

65. Oner, D.; McCarthy, T. J., Ultrahydrophobic surfaces. Effects of topography length scales on wettability. *Langmuir* **2000,** *16* (20), 7777-7782.

66. Garbassi, F.; Morra, M.; Occhiello, E., *Polymer surfaces from physics to technology*. Wiley: Chichester ; New York, 1994; p ix, 462 p.

67. Chen, X.; Hutchinson, J. W., Herringbone buckling patterns of compressed thin films on compliant substrates. *J Appl Mech-T Asme* **2004,** *71* (5), 597-603.

68. Ohzono, T.; Shimomura, M., Ordering of microwrinkle patterns by compressive strain. *Phys Rev B* **2004,** *69* (13).

69. Huck, W. T. S.; Bowden, N.; Onck, P.; Pardoen, T.; Hutchinson, J. W.; Whitesides, G. M., Ordering of spontaneously formed buckles on planar surfaces. *Langmuir* **2000,** *16* (7), 3497-3501.

70. Bowden, N.; Brittain, S.; Evans, A. G.; Hutchinson, J. W.; Whitesides, G. M., Spontaneous formation of ordered structures in thin films of metals supported on an elastomeric polymer. *Nature* **1998,** *393* (6681), 146-149.

71. Ohzono, T.; Matsushita, S. I.; Shimomura, M., Coupling of wrinkle patterns to microsphere-array lithographic patterns. *Soft Matter* **2005,** *1* (3), 227-230.

72. Efimenko, K.; Rackaitis, M.; Manias, E.; Vaziri, A.; Mahadevan, L.; Genzer, J., Nested self-similar wrinkling patterns in skins. *Nat Mater* **2005,** *4* (4), 293-297.

73. Tserepi, A.; Gogolides, E.; Tsougeni, K.; Constantoudis, V.; Valamontes, E. S., Tailoring the surface topography and wetting properties of oxygen-plasma treated polydimethylsiloxane. *J Appl Phys* **2005,** *98* (11).

74. Tsougeni, K.; Boulousis, G.; Gogolides, E.; Tserepi, A., Oriented spontaneously formed nano-structures on poly(dimethylsiloxane) films and stamps treated in O-2 plasmas. *Microelectron Eng* **2008,** *85* (5-6), 1233-1236.

75. Moon, M. W.; Vaziri, A., Surface modification of polymers using a multi-step plasma treatment. *Scripta Mater* **2009,** *60* (1), 44-47.

76. Suresh, S., Biomechanics and biophysics of cancer cells. *Acta Biomater* **2007,** *3* (4), 413-438.

77. Bao, G.; Suresh, S., Cell and molecular mechanics of biological materials. *Nat Mater* **2003,** *2* (11), 715-725.

78. Pullarkat, P. A.; Fernandez, P. A.; Ott, A., Rheological properties of the Eukaryotic cell cytoskeleton. *Phys Rep* **2007,** *449* (1-3), 29-53.

79. Pines, M.; Oplinger, A. A.; National Institute of General Medical sciences (U.S.), *Inside the cell*. U.S. Dept. of Health and Human Services, Public Health Service, National Institutes of Health, National Institute of General Medical Sciences: Bethesda, Md.?, 1990; p 62 p.

80. Owen, S. C.; Shoichet, M. S., Design of three-dimensional biomimetic scaffolds. *J Biomed Mater Res A* **2010,** *94A* (4), 1321-1331.

81. Discher, D. E.; Janmey, P.; Wang, Y. L., Tissue cells feel and respond to the stiffness of their substrate. *Science* **2005,** *310* (5751), 1139-1143.

82. Geiger, B.; Bershadsky, A.; Pankov, R.; Yamada, K. M., Transmembrane extracellular matrix-cytoskeleton crosstalk. *Nat Rev Mol Cell Bio* **2001,** *2* (11), 793-805.

83. Cretel, E.; Touchard, D.; Benoliel, A. M.; Bongrand, P.; Pierres, A., Early contacts between T lymphocytes and activating surfaces. *J Phys-Condens Mat* **2010,** *22* (19).

84. Vogel, V.; Sheetz, M., Local force and geometry sensing regulate cell functions. *Nat Rev Mol Cell Bio* **2006,** *7* (4), 265-275.

85. Vladkova, T. G., Surface Engineered Polymeric Biomaterials with Improved Biocontact Properties. *Int J Polym Sci* **2010**.

86. Lanza, R. P.; Langer, R. S.; Chick, W. L., *Principles of tissue engineering*. Academic Press ;

R.G. Landes: San Diego

Austin, 1997; p 808 p.

87. Holl, M. B., Polymer interactions with the cell plasma membrane. *Abstr Pap Am Chem S* **2009,** *237*.

88. Grayson, A. C. R.; Shawgo, R. S.; Johnson, A. M.; Flynn, N. T.; Li, Y. W.; Cima, M. J.; Langer, R., A BioMEMS review: MEMS technology for physiologically integrated devices. *P Ieee* **2004,** *92* (1), 6-21.

89. Rovensky, Y. A.; Slavnaja, I. L.; Vasiliev, J. M., Behaviour of Fibroblast-Like Cells on Grooved Surfaces. *Exp Cell Res* **1971,** *65* (1), 193-&.

90. Weiss, P., In vitro experiments on the factors determining the course of the outgrowing nerve fiber. *Exp Zool* **1934,** *69*, 393-448.

91. Teixeira, A. I.; Abrams, G. A.; Bertics, P. J.; Murphy, C. J.; Nealey, P. F., Epithelial contact guidance on well-defined micro- and nanostructured substrates. *J Cell Sci* **2003,** *116* (10), 1881-1892.

92. denBraber, E. T.; deRuijter, J. E.; Smits, H. T. J.; Ginsel, L. A.; vonRecum, A. F.; Jansen, J. A., Quantitative analysis of cell proliferation and orientation on substrata with uniform parallel surface micro-grooves. *Biomaterials* **1996,** *17* (11), 1093-1099.

93. denBraber, E. T.; deRuijter, J. E.; Ginsel, L. A.; vonRecum, A. F.; Jansen, J. A., Quantitative analysis of fibroblast morphology on microgrooved surfaces with various groove and ridge dimensions. *Biomaterials* **1996,** *17* (21), 2037-2044.

94. den Braber, E. T.; de Ruijter, J. E.; Ginsel, L. A.; von Recum, A. F.; Jansen, J. A., Orientation of ECM protein deposition, fibroblast cytoskeleton, and attachment complex components on silicone microgrooved surfaces. *J Biomed Mater Res* **1998,** *40* (2), 291-300.

95. denBraber, E. T.; deRuijter, J. E.; Jansen, J. A., The effect of a subcutaneous silicone rubber implant with shallow surface microgrooves on the surrounding tissues in rabbits. *J Biomed Mater Res* **1997,** *37* (4), 539-547.

96. Walboomers, X. F.; Monaghan, W.; Curtis, A. S. G.; Jansen, J. A., Attachment of fibroblasts on smooth and microgrooved polystyrene. *J Biomed Mater Res* **1999,** *46* (2), 212-220.

97. Alaerts, J. A.; De Cupere, V. M.; Moser, S.; de Aguilar, P. V. B.; Rouxhet, P. G., Surface characterization of poly(methyl methacrylate) microgrooved for contact guidance of mammalian cells. *Biomaterials* **2001,** *22* (12), 1635-1642.

98. Lenhert, S.; Sesma, A.; Hirtz, M.; Chi, L. F.; Fuchs, H.; Wiesmann, H. P.; Osbourn, A. E.; Moerschbacher, B. M., Capillary-induced contact guidance. *Langmuir* **2007,** *23* (20), 10216-10223.

99. Dalby, M. J.; Riehle, M. O.; Yarwood, S. J.; Wilkinson, C. D. W.; Curtis, A. S. G., Nucleus alignment and cell signaling in fibroblasts: response to a micro-grooved topography. *Exp Cell Res* **2003,** *284* (2), 274-282.

100. Zhou, X. T.; Shi, J.; Hu, J.; Chen, Y., Cells cultured on microgrooves with or without surface coating: Correlation between cell alignment, spreading and local membrane deformation. *Mat Sci Eng C-Mater* **2013,** *33* (2), 855-863.

101. Cheng, W. H.; He, L.; Fan, X. X.; Ou, Q. R.; Liang, R. Q., Surface modification of indium tin oxide by oxygen plasma immersion ion implantation. *Sci China Technol Sc* **2013,** *56* (4), 925-929.

102. Lu, T.; Qiao, Y. Q.; Liu, X. Y., Surface modification of biomaterials using plasma immersion ion implantation and deposition. *Interface Focus* **2012,** *2* (3), 325-336.

103. Zhu, X.; Chian, K. S.; Chan-Park, M. B. E.; Lee, S. T., Effect of argon-plasma treatment on proliferation of human-skin-derived fibroblast on chitosan membrane in vitro. *J Biomed Mater Res A* **2005,** *73A* (3), 264-274.

104. Bazaka, K.; Jacob, M. V.; Crawford, R. J.; Ivanova, E. P., Plasma-assisted surface modification of organic biopolymers to prevent bacterial attachment. *Acta Biomater* **2011,** *7* (5), 2015-2028.

105. Wang, J.; Huang, N.; Yang, P.; Leng, Y.; Sun, H.; Liu, Z. Y.; Chu, P. K., The effects of amorphous carbon films deposited on polyethylene terephthalate on bacterial adhesion. *Biomaterials* **2004,** *25* (16), 3163-3170.

106. Liu, C. Z.; Meenan, B. J., Effect of Air Plasma Processing on the Adsorption Behaviour of Bovine Serum Albumin on Spin-Coated PMMA Surfaces. *J Bionic Eng* **2008,** *5* (3), 204-214.

107. Qi, L.; Li, N.; Huang, R.; Song, Q.; Wang, L.; Zhang, Q.; Su, R. G.; Kong, T.; Tang, M. L.; Cheng, G. S., The Effects of Topographical Patterns and Sizes on Neural Stem Cell Behavior. *Plos One* **2013,** *8* (3).

108. D'Sa, R. A.; Burke, G. A.; Meenan, B. J., Protein adhesion and cell response on atmospheric pressure dielectric barrier discharge-modified polymer surfaces. *Acta Biomater* **2010,** *6* (7), 2609-2620.

109. Chu, P. K., Progress in direct-current plasma immersion ion implantation and recent applications of plasma immersion ion implantation and deposition. *Surf Coat Tech* **2013,** *229*, 2-11.

110. Zeng, X. C.; Fu, R. K. Y.; Kwok, D. T. K.; Chu, P. K., Quasi-direct current plasma immersion ion implantation. *Appl Phys Lett* **2001,** *79* (19), 3044-3046.

111. Wang, H. Y. K., D. T. K.; Wang, W.; Wu, Z. W.; Tong, L. P.; Zhang, Y. M.; Chu, P. K. , Osteoblast behavior on polytetrafluoroethylene modified by long pulse, high frequency oxygen plasma immersion ion implantation. *Biomaterials* **2009,** *doi:10.1016/j.biomaterials.2009.09.066*.

112. Xu, R. Z.; Yang, X. B.; Suen, K. W.; Wu, G. S.; Li, P. H.; Chu, P. K., Improved corrosion resistance on biodegradable magnesium by zinc and aluminum ion implantation. *Appl Surf Sci* **2012,** *263*, 608-612.

113. Wang, J.; Pan, C. J.; Kwok, S. C. H.; Yang, P.; Chen, J. Y.; Wan, G. J.; Huang, N.; Chu, P. K., Characteristics and anticoagulation behavior of polyethylene terephthalate modified by C2H2 plasma immersion ion implantation-deposition. *J Vac Sci Technol A* **2004,** *22* (1), 170-175.

114. http://en.wikipedia.org/wiki/File:Atomic_force_microscope_block_diagram.svg.

115. http://en.wikipedia.org/wiki/File:AFM_(used)_cantilever_in_Scanning_Electron_Microscope,_magnification_1000x.JPG.

116. Jandt, K. D., Atomic force microscopy of biomaterials surfaces and interfaces. *Surf Sci* **2001,** *491* (3), 303-332.

117. Braga, P. C.; Ricci, D., *Atomic force microscopy in biomedical research : methods and protocols*. Humana Press: New York, 2011; p xiv, 508 p.

118. Bonnell, D. A., *Scanning probe microscopy and spectroscopy : theory, techniques, and applications*. 2nd ed.; Wiley-VCH: New York, 2001; p xiv, 493 p.

119. Poole, C. P.; Owens, F. J., *Introduction to nanotechnology*. J. Wiley: Hoboken, NJ, 2003; p xii, 388 p.

120. Bandhyopadhya, A.; Bose, S., *Characterization of biomaterials*. p xii, 437 pages.

121. Jackman, H.; Krakhmalev, P.; Svensson, K., Image formation mechanisms in scanning electron microscopy of carbon nanotubes, and retrieval of their intrinsic dimensions. *Ultramicroscopy* **2013,** *124*, 35-39.

122. Hobart, K. D.; Kub, F. J.; Fatemi, M.; Twigg, M. E.; Thompson, P. E.; Kuan, T. S.; Inoki, C. K., Compliant substrates: A comparative study of the relaxation mechanisms of strained films bonded to high and low viscosity oxides. *J Electron Mater* **2000,** *29* (7), 897-900.

123. Kwon, S. J.; Yoo, P. J.; Lee, H. H., Wave interactions in buckling: Self-organization of a metal surface on a structured polymer layer. *Appl Phys Lett* **2004,** *84* (22), 4487-4489.

124. Biot, M. A., *Mechanics of incremental deformations; theory of elasticity and viscoelasticity of initially stressed solids and fluids, including thermodynamic foundations and applications to finite strain*. Wiley: New York,, 1965; p xvii, 504 p.

125. Landau, L. D.; Lifshi͡ts, E. M., *Teoriĭa uprugosti*. 1965; p 202 p.

126. Timoshenko, S., *Theory of elastic stability*. 2d ed.; McGraw-Hill: New York,, 1961; p 541 p.

127. Brush, D. O.; Almroth, B. O., *Buckling of bars, plates, and shells*. McGraw-Hill: New York,, 1975; p xvii, 379 p.

128. Allen, H. G., *Analysis and design of structural sandwich panels*. 1st ed.; Pergamon Press: Oxford, New York,, 1969; p xvi, 283 p.

129. Genzer, J.; Groenewold, J., Soft matter with hard skin: From skin wrinkles to templating and material characterization. *Soft Matter* **2006,** *2* (4), 310-323.

130. Burton, K.; Taylor, D. L., Traction forces of cytokinesis measured with optically modified elastic substrata. *Nature* **1997,** *385* (6615), 450-454.

131. D., H. A. K. W. P. S., silicon rubber substrata: a new wrinkle in the study of cell locomotion. *science* **1980,** *208* (4440), 177-179.

132. Kong, H. J.; Liu, J. D.; Riddle, K.; Matsumoto, T.; Leach, K.; Mooney, D. J., Non-viral gene delivery regulated by stiffness of cell adhesion substrates. *Nat Mater* **2005,** *4* (6), 460-464.

133. Ulrich, T. A.; Pardo, E. M. D.; Kumar, S., The Mechanical Rigidity of the Extracellular Matrix Regulates the Structure, Motility, and Proliferation of Glioma Cells. *Cancer Res* **2009,** *69* (10), 4167-4174.

134. Tibbitt, M. W.; Anseth, K. S., Hydrogels as Extracellular Matrix Mimics for 3D Cell Culture. *Biotechnol Bioeng* **2009,** *103* (4), 655-663.

135. Aubin, H.; Nichol, J. W.; Hutson, C. B.; Bae, H.; Sieminski, A. L.; Cropek, D. M.; Akhyari, P.; Khademhosseini, A., Directed 3D cell alignment and elongation in microengineered hydrogels. *Biomaterials* **2010,** *31* (27), 6941-6951.

136. Kim, D. H.; Lipke, E. A.; Kim, P.; Cheong, R.; Thompson, S.; Delannoy, M.; Suh, K. Y.; Tung, L.; Levchenko, A., Nanoscale cues regulate the structure and function of macroscopic cardiac tissue constructs. *P Natl Acad Sci USA* **2010,** *107* (2), 565-570.

137. Gittens, R. A.; McLachlan, T.; Olivares-Navarrete, R.; Cai, Y.; Berner, S.; Tannenbaum, R.; Schwartz, Z.; Sandhage, K. H.; Boyan, B. D., The effects of combined micron-/submicron-scale surface roughness and nanoscale features on cell proliferation and differentiation. *Biomaterials* **2011,** *32* (13), 3395-3403.

138. Eslaminejad, M. B.; Bagheri, F.; Zandi, M.; Nejati, E.; Zomorodian, E., Study of Mesenchymal Stem Cell Proliferation and Bone Differentiation on Composite Scaffolds of PLLA and Nano Hydroxyapatite with Different Morphologies. *Yakhteh* **2011,** *12* (4), 469-476.

139. Uttayarat, P.; Toworfe, G. K.; Dietrich, F.; Lelkes, P. I.; Composto, R. J., Topographic guidance of endothelial cells on silicone surfaces with micro- to nanogrooves: Orientation of actin filaments and focal adhesions. *J Biomed Mater Res A* **2005,** *75A* (3), 668-680.

140. Zhu, B. S.; Lu, Q. H.; Yin, J.; Hu, J.; Wang, Z. G., Alignment of osteoblast-like cells and cell-produced collagen matrix induced by nanogrooves. *Tissue Eng* **2005,** *11* (5-6), 825-834.

141. Khorasani, M. T.; MoemenBellah, S.; Mirzadeh, H.; Sadatnia, B., Effect of surface charge and hydrophobicity of polyurethanes and silicone rubbers on L929 cells response. *Colloid Surface B* **2006,** *51* (2), 112-119.

142. Ricci, J. L. C., J.; Chang, R.; Howard, C., In Vitro Effects of Surface Microgeometry on Colony Formation by Fibroblasts and Bone Cells. *20th annual meeting of the society for biomaterials, Bosten, USA* **1994**.

143. Green, A. M.; Jansen, J. A.; Vanderwaerden, J. P. C. M.; Vonrecum, A. F., Fibroblast Response to Microtextured Silicone Surfaces - Texture Orientation into or out of the Surface. *J Biomed Mater Res* **1994,** *28* (5), 647-653.

144. Ismailoglu, U. B.; Saracoglu, I.; Harput, U. S.; Sahin-Erdemli, I., Effects of phenylpropanoid and iridoid glycosides on free radical-induced impairment of endothelium-dependent relaxation in rat aortic rings. *J Ethnopharmacol* **2002,** *79* (2), 193-197.

145. Navarro-Antolin, J.; Lopez-Munoz, M. J.; Soria, J.; Lamas, S., Superoxide limits cyclosporine-A-induced formation of peroxynitrite in endothelial cells. *Free Radical Bio Med* **2002,** *32* (8), 702-711.

146. Aslan, M.; Freeman, B. A., Redox-dependent impairment of vascular function in sickle cell disease. *Free Radical Bio Med* **2007,** *43* (11), 1469-1483.

147. Zhang, X. H.; Matsuda, N.; Jesmin, S.; Sakuraya, F.; Gando, S.; Kemmotsu, O.; Hattori, Y., Normalization by edaravone, a free radical scavenger, of irradiation-reduced endothelial nitric oxide synthase expression. *Eur J Pharmacol* **2003,** *476* (1-2), 131-137.

148. Feinberg, A. W.; Schumacher, J. F.; Brennan, A. B., Engineering high-density endothelial cell monolayers on soft substrates. *Acta Biomater* **2009,** *5* (6), 2013-2024.

149. Chung, S. H.; Min, J., Morphological investigations of cells that adhered to the irregular patterned polydimethylsiloxane (PDMS) surface without reagents. *Ultramicroscopy* **2009,** *109* (8), 861-867.

150. Samaroo, H. D.; Lu, J.; Webster, T. J., Enhanced endothelial cell density on NiTi surfaces with sub-macron to nanometer roughness. *Int J Nanomed* **2008,** *3* (1), 75-82.

151. Castleman, L. S.; Motzkin, S. M.; Alicandri, F. P.; Bonawit, V. L.; Johnson, A. A., Biocompatibility of Nitinol Alloy as an Implant Material. *J Biomed Mater Res* **1976,** *10* (5), 695-731.

152. Sui, J. H.; Cai, W., Effect of diamond-like carbon (DLC) on the properties of the NiTi alloys. *Diam Relat Mater* **2006,** *15* (10), 1720-1726.

153. Kobayashi, S.; Ohgoe, Y.; Ozeki, K.; Sato, K.; Sumiya, T.; Hirakuri, K. K.; Aoki, H., Diamond-like carbon coatings on orthodontic archwires. *Diam Relat Mater* **2005,** *14* (3-7), 1094-1097.

154. Clarke, B.; Carroll, W.; Rochev, Y.; Hynes, M.; Bradley, D.; Plumley, D., Influence of nitinol wire surface treatment on oxide thickness and composition and its subsequent effect on corrosion resistance and nickel ion release. *J Biomed Mater Res A* **2006,** *79A* (1), 61-70.

155. Ryhanen, J.; Kallioinen, M.; Tuukkanen, J.; Junila, J.; Niemela, E.; Sandvik, P.; Serlo, W., In vivo biocompatibility evaluation of nickel-titanium shape memory metal alloy: Muscle and perineural tissue responses and encapsule membrane thickness. *J Biomed Mater Res* **1998,** *41* (3), 481-488.

156. Lu, X. Y.; Bao, X.; Huang, Y.; Qu, Y. H.; Lu, H. Q.; Lu, Z. H., Mechanisms of cytotoxicity of nickel ions based on gene expression profiles. *Biomaterials* **2009,** *30* (2), 141-148.

157. Firstov, G. S.; Vitchev, R. G.; Kumar, H.; Blanpain, B.; Van Humbeeck, J., Surface oxidation of NiTi shape memory alloy. *Biomaterials* **2002,** *23* (24), 4863-4871.

158. Baviskar, S. N., A Quick & Automated Method for Measuring Cell Area Using ImageJ. *Am Biol Teach* **2011,** *73* (9), 554-556.

159. Weiss, P., Experiments on cell and axon orientation in vitro: The role of colloidal exudates in tissue organization. *Exp Zool* **1945,** *100*, 353-386.